A PHOTOIONIZATION COINCIDENCE TIME-OF-FLIGHT MASS SPECTROMETER FOR STUDIES ON IONIZATION AND DISSOCIATION PROCESSES

A thesis presented for the degree of

DOCTOR OF PHILOSOPHY

to

The University of Glasgow

by

MARIA DE LOURDES FRASER MONTEIRO

JULY, 1969.

ProQuest LLC.
789 East Eisenhower Parkway
P.O. Box 1346
Ann Arbor, MI 48106 – 1346

To

ANDRE and ANTONIA

born during the progress of this work

C O N T E N T S

Acknowledgements

CHAPTER 1. INTRODUCTION

A Brief History of the Development of the Mass Spectrometer 1

References 19

CHAPTER 2. DESCRIPTION OF THE APPARATUS AND EXPERIMENTAL PROCEDURE 22

2.1 - Vacuum system 23

2.2 - Inlet System 27

2.3 - Light source 29

2.4 - Photon detector 35

2.5 - Assembly of the ion and electron accelerators with the respective ion and electron detectors 36

2.6 - Electronic units and circuitry 45

References 51

CHAPTER 3. THEORETICAL CONSIDERATIONS

3.1 - Photoionization processes 53

3.2 - Coincidence technique 59

3.3 - Travel time of ions and resolution 65

3.4 - The application of the coincidence time-of-flight mass spectrometer to direct determinations of metastable ion life-times 73

References 79

CHAPTER 4. EXPERIMENTAL RESULTS AND DISCUSSION 81

ACKNOWLEDGEMENTS

The author's deepest gratitude goes to her supervisor, Dr.R.I.Reed, for the unceasing support he gave to this project and for his unsurpassing confidence in its success, even at those gloomy times when, through the accum ulation of many, unsuspected and multifarious faults of the equipment, this failed to produce the faintest response to our efforts.

She is very much indebted to her husband, L.Fraser Monteiro, for his constant and constructive criticism , during all the phases of the work.

The devotion, infinite patience and high standard of craftsmanship of Mr.A.Harvey of the Department's mechanical workshop was one of the main factors that made this work possible.

Thanks are also due to the very competent team of the glassblowing workshop, led by Mr.J.Connolly, that made several models of the light lamp and assembled the inlet system.

The help of Mr.A.Leven and Mr.J.Hardy in several practical electronics problems is also gratefully acknowledged.

We are indebted to the Atomic Weapons Research Establishment, Aldermaston, Berks., in particular to Dr.N.Daly, for the use of the two amplifiers. Also to Mr.W.A.P.Young, of the same Establishment, for his keen interest and very valuable advice.

We also acknowledge MrR.Hutchins and Mr.J.A.Bennett, of the Department of Electrical Engineering, for baking all the pyrophyllite parts; Mr.W.B.Askew, of E.I.du Pont de Nemours & Co., Delaware, for supplying the sample of 1,1,1-trifluoroethane; Dr.G.Webb, for the handling of the gaseous samples; Rolls Royce Ltd., East Kilbride, for having argon-arc welded the stainless steel tubes; Miss A.Tennent and Mr.A.Maclean for technical assistance.

Last,not least, the friendly and cordial atmosphere among all the colleagues of the group is gratefully remembered.

Chapter One

INTRODUCTION
A BRIEF HISTORY OF THE DEVELOPMENT OF THE MASS SPECTROMETER

A mass spectrometer (or spectrograph) is an instrument able to differentiate between gaseous ions with respect to their mass-to-charge ratio.

If, for the detection of ions, a photographic plate is used, the term spectrograph is common; when the detection is made by electrical means, the name mass spectrometer generally is used.

The first instrument capable of separating the mass components of a given chemical element was built by J. J. Thomson [1] in 1907. In this apparatus a beam of positively charged particles is subjected to the combined action of electric and (parallel\magnetic) fields. For each mass-to-charge ratio, Thomson obtained on a photographic plate a truncated parabolic curve. A spot image for each mass would have resulted but for the large energy spread of the ions, produced by an electric discharge.

Even so, he could demonstrate that neon consisted of two atomic species, one of atomic mass 20 and the other of

atomic mass 22.

This observation of the existence of stable isotopes is one of the greatest achievements claimed by mass spectroscopy.

In 1919, F.W. Aston [2] built another type of instrument which produced a line spectrum on a photographic plate, each line corresponding to a particular mass-to-charge ratio.

The ions, after being found, passed through electric and magnetic fields and arranged in succession in a way that the dispersion caused by the electric field is compensated by the focusing properties produced by that of the magnet.

Thus, although the positive ions with the same mass-to-charge ratio come into the magnetic analyser with a big range of velocities and so follow different paths, they are focused in the same line in a photographic plate. This action is called "velocity focusing".

For the identification of the masses, Aston used a standard mass and noted its position in the photographic plate and the unknown masses were deduced by empirical relations to it. Many errors were involved in that process. The focusing was not perfect and because at the time the relation between the density of blackening of the plates and the beam intensity was unknown, it was not possible to make relative abundance measurements.

However, Aston made a systematic search for isotopes in more than 50 of the light elements.

At the same time, Dempster [3] developed another type of mass spectrometer in which the positive ions, after being accelerated in an electric field, were passed through a slit and deflected through 180° arc by a magnetic field placed perpendicular to the direction of motion of the ions which in consequence describe a circle of radius r such that the centrifuge force equals the magnetic force,

$$\text{i.e.} \qquad m\frac{v^2}{r} = Bev \qquad (1)$$

where m is the ion mass, v the ion velocity, e the ion electric charge and B the magnetic induction.

The radius r of the trajectory is proportioned to the momentum of the particle.

If the original kinetic energy of the ions is negligible in comparison with the energy obtained by acceleration in the electric field, we have

$$\frac{1}{2}mv^2 = eV \qquad (2)$$

where V is the accelerating voltage.

Eliminating v between (1) and (2)

$$\frac{m}{e} = \frac{r^2B^2}{2V} \qquad (3)$$

in which the radius of the trajectory is proportional to

to the square root of the mass-to-charge ratio $\frac{m}{e}$, and then the spectrum of momentum becomes a mass spectrum.

The ions are focused in a plane after passing through the magnetic field, owing to the properties of directional focusing of the magnetic fields. [4,5,6.] Hence the name "direction focusing spectrometer" given to the Dempster machine.

As he used electrical means of recording the ion beam, relative abundance measurements were possible.

In 1932, Bleakney [7] described another spectrometer also of 180° deflection in which the magnetic field for the ion analysis was produced by a solenoid.

Until 1940, all the mass spectrometers produced were of one of these two types; Dempster or Bleakney, i.e. all of 180° of arc deflection.

The spectrometers that combine "velocity focusing" and "direction focusing" are termed "double focusing spectrometers" Their general theory was deduced by Herzog [4] and the design

of Mattauch and Herzog [8] is still widely used. However, some of the modern "double-focusing mass spectrometers" use the Johnson and Nier design which is more amenable to measuring the abundance of any given ion. These mass spectrometers are capable of much higher resolution than the single focusing instruments, as the combination of electric and magnetic fields compensates for the energy spread of the ions when they leave the ion source.

In 1940, Nier [9] published the details of the first "sector field direction focusing instrument" having a 60^{o} of arc sector for the magnetic deflection. In 1942, Hipple [10] described a 90^{o} sector field instrument and nowadays most of the sector field magnetic deflection spectrometers are one or other of these.

Additionally, there is the cycloidal-focusing mass spectrometer first produced by Bleakney and Hipple [11], in which a beam of ions diverging from a source slit is de: :flected by crossed electric and magnetic fields.

Ions of a given $\frac{m}{e}$ ratio converge to a focus, after describing different cycloidal trajectories.

One of the advantages of this design consists on its relative insensitivity both to energy spread and angular divergence of the ion beam. The instrument is mainly used for gas analysis in the mass range 12 to 150 a.m.u.

Radio-frequency mass spectrometers were first reported by Smyth and Mattauch.[12,13] However, the present models were described by Bennett.[14] In these instruments an ion beam homogeneous in energy passes through a succession of radio-frequency stages separated by field-free drift speces. Those with an appropriate velocity are preferentially accelerated and can overcome a static retarding field, while ions having other velocities are rejected. Because of the homogenity in energy of the ion beam, the velocity of an ion is characteristic of its mass then the velocity analysis achieved in the spectrometer is equivalent to mass analysis. An advantage of the radio-frequency mass spectrometer is that it requires no magnet. The analyser is compact and its construction is simplified by the fact that there are no

slits to be aligned. Although the resolving power is modest the instrument is useful for the analysis of gases in the upper atmosphere.

A further type of apparatus is the time-of-flight mass spectrometer, first reported by Cameron and Eggers [15] and subsequently by many other workers [16-19]. The ions formed by electron impact with a pulsed beam of electrons are accelerated through an electric field and projected along a field-free space towards a detector. The time interval between the pulse of the electron beam and the pulse produced in the ion detector by the arrival of a bunch of ions is a function of the mass-to-charge ratio of the ions.

The mass resolution obtained with this spectrometer depends on the spread of the flight times for ions of the same mass-to-charge ratio.

This spread must not exceed the difference in travel times for adjacent masses if those are to be resolved.

This instrument is valuable for monitoring high speed

reactions as the repetitive scan rate may be as high as 20000 cycles/second. With some modifications [20] that comprise the introduction of a retarding field barrier in the field-free drift tube, before the collector this apparatus has been used both for studies in ion dissociation [21] [22] and charge transfer processes [23].

Paul and co-workers [24,25,26] developed a quadrupole mass spectrometer in which the mass separation is done in an quadrupolar radio-frequency field. The ion beam travels through the axis of the quadrupole field which is produced by four parallel cylindrical rods to which there is applied a dc-potential with a superimposed high frequency voltage. The ions perform oscillations perpendicular to the travel axis which remain below a maximum permitted amplitude only for a certain mass range of ions. Therefore, only these ions can pass through the quadrupole field and all other ions performing unstable oscillations with rapidly rising amplitudes strike the rod electrodes or escape

between them and are lost to the system. The advantages of the instrument include the absence of a magnet and so the analyser tube is light. Actually its major use is in the analysis of residual gases but it is also widely used as a mass filter of high transmittance as it is without slits.

Sommer, Thomas and Hipple [27] devised an apparatus, the "Omegatron", which employs a magnetic field crossed with a radio-frequency field to scan the mass spectrum. The ions in resonance with the radio-frequency field describe a growing spiral gaining energy in each half-revolution as in the operation of a cyclotron. The out-of-phase ions lose energy and are not able to reach the collector. Because of the rather long ion path this instrument requires a very high vacuum, so its main use is residual gas analysis in high vacuum systems.

In general, we can say that the first mass spectrometers built had as primary aims the determination of ion masses for the identification of substances and measurement of

relative isotopic abundances.

Then the mass spectrometer became a useful tool in the analysis of hydrocarbons and still continues to be of great value in the identification and quantitative analysis of mixtures of these [28].

Later, the mass spectrometer, besides continuing as an indispensable analytical tool, has had its applications extended to include studies of molecular structure, chemical kinetics, determination of dissociation energies, ionization and appearance potentials, latent heats of sublimation, reaction mechanisms by isotopic labeling techniques, etc.

In recent years, mass spectromers have been designed and built for pure research purposes, notably for studies on ionization and dissociation processes [29,30] and for increasing our information about the upper energy states of molecules.[31-33]

In all, the mass spectrometers already described,

only the positive ions produced in the ion source are collected and analysed, while the ejected electrons are ignored.

Rosenstock in 1961 [34] described a coincidence time-of-flight mass spectrometer in which both the secondary electron and the positive ion produced by electron impact ionization are collected. The time interval between collection of a secondary electron and the corresponding positive ion is an accurate measure of the mass-to- charge ratio of this ion.

The coincidence mass spectrometer is particularly important in studies of ionization and dissociation processes as a single ionization event can be detected separately.

For example, Rosenstock et al [35] used this apparatus successfully for direct observation of the decomposition of multiply charged ions into singly charged fragments.

The method of ionization generally used in most mass spectrometers is the bombardment by nearly monoenergetic electrons of about 50-70 ev energy, produced by thermionic emission from a hot filament.

A molecule in the gaseous state is bombarded by an

electron, producing a positive ion and ejecting another electron,

$$AB + e^- \rightarrow AB^+ + e^- + e^-$$

Owing to the ample excess energy of the electrons over the ionization potentials of the molecules in study, many secondary decompositions of the molecular ions take place, many inside the ion chamber, others in transit to the collector. Therefore, a very complex spectrum generally results. Simpler spectra are produced if the ionization is induced by the methods of field ionization, chemical ionization or photon impact.

The simpler form of photoionization is described by

$$h\nu + AB \longrightarrow AB^+ + e^-$$

Nearly monochromatic photon beams have been used for many years [36] to study photoionization processes in low pressure gaseous systems but, except for the early

experiments of Terenin and Popov [37], not until 1956, (Lossing and Tanaka [38]) was photoionization used for the first time in an ion source in mass spectrometry.

In none of these experiments the photon energy could be varied continuously for studies of the photoionization yield vs the photon energy.

Hurzeler, Inghram and Morrison [29] were the first to combine a vacuum ultraviolet monochromator attached to a mass spectrometer to study photoionization processes.

The advantages of photoionization over electron impact are many:

1. It is much easier to get a monochromatic beam of photons with a strictly controlled energy than of electrons. Thus, for example, with ordinary vacuum monochromators one can easily obtain a resolution of the order of 1A°, which corresponds to a scatter of photon energies of the order of 0.01 ev.

2. In photoionization, the ion current near the appearance threshold of the ions rises very sharply, in comparison with ionization by electron impact, and so allows a better understanding of the ion formation processes. This difference in the shapes of the

photoionization and electron impact efficiency curves is explained by the fact that the ionizing electrons, having spent their energy in ionization and in imparting a certain excitation to the ions, remain in their vicinity and can neutralize them . The ionization yield increases only when the excess kinetic energy becomes large enough so that the electron and the ion separate quickly.

3. Photoionization gives more detailed information of ionization, auto-ionization and fragmentation of ions.

4. It is more suitable for quantitative work as it avoids the difficulties arising from contact potentials which are associated with electron impact sources.

5. Owing to the absence of a hot filament, pyrolisis of sensitive substances is avoided and, consequently, a higher pressure may be employed in the source, limited only by the pressure in the analyser.

There are also some disadvantages. First, it is difficult to get intense continuum sources in the

vacuum ultraviolet and, second, relatively weak ion beams are obtained.

However, owing to the above advantages, photoionization is becoming a more widespread method of producing ions. Initially, the photon energy used was limited by the absorption in the window inserted between the light source and the ionization chamber. Lossing and Tanaka,[38] Herzog and Marmo [39] and Morrison, Hurzeler and Inghram [29] used lithium fluoride windows and so wavelengths below 1050 A^{o} were completely absorbed. Hence the compounds that could be ionized were limited to those with ionization potentials less than 11.8 ev.

Later, this limitation was removed [30,40,41] by eliminating the window, but in view of the pressure used in the lamp (1 torr minimum) a high degree of differential pumping is necessary to keep the high vacuum in the analyser.

We undertook to build a time-of-flight mass

spectrometer in which the advantages of the coincidence technique are combined with those from using photoionization. Its design and construction were for the development of studies on ionization and dissociation processes, including direct observation of metastable decompositions. It can also admit determinations of the energy distribution of the photo-electrons ejected and, consequently, determinations on the ion energy levels.

REFERENCES

1. J.J.THOMSON, Phil.Mag., 13 (1907) 561.

2. F.W.ASTON, Phil.Mag., 38 (1919) 707 and 709.

3. A.J.DEMPSTER, Phys.Rev., 11 (1918) 316.

4. R.HERZOG, Z.Physik, 89 (1934) 447, 786.

5. N.F.BARBER, Proc.Leeds Phil.Lit.Soc., 2 (1933) 427.

6. W.E.STEPHENS, Phys.Rev., 45 (1934) 513.

7. W.BLEAKNEY, Phys.Rev., 40 (1932) 496.

8. J.MATTAUCH and R.HERZOG, Z.Physik, 89 (1934) 786.

9. A.O.NIER, Rev.Sci.Instr., 11 (1940) 212.

10. A.J.HIPPLE, J.Appl.Phys., 13 (1942) 551; A.J.HIPPLE, D.GROVE and W.HICKAM, Rev.Sci.Instr., 16 (1945) 69.

11. W.BLEAKNEY and J.A.HIPPLE, Phys.Rev., 53 (1938) 521.

12. W.R.SMITH and J.MATTAUCH, Phys.Rev., 40 (1932) 429.

13. W.R.SMITH, Phys.Rev., 45 (1934) 299.

14. W.H.BENNETT, J.Appl.Phys., 21 (1950) 143.

15. A.E.CAMERON and D.F.EGGERS, Rev.Sci.Instr., 19 (1948) 605.

16. R.KELLER, Helv.Phys.Acta, 22 (1949) 386.

17. M.M.WOLFF and W.E.STEPHENS, Rev.Sci.Instr., 24 (1953) 616.

18. H.S.KATZENSTEIN and SS.FRIEDLAND, Rev.Sci.Instr., 26 (1955)324.

19. W.C.WILEY and I.H.McLAREN, Rev.Sci.Instr., 26 (1955) 1150.

20. W.W.HUNT,Jr., R.E.HUFFMAN, J.SAARI, G.WASSEL, J.F.BETTS, E.H.PAUFVE, W.WYESS and R.A.FLUEGGE, Rev.Sci.Instr., 35 (1964) 88.

21. W.W.HUNT,Jr., R.E.HUFFMAN and K.E.McGEE, Rev.Sci.Instr., 35 (1964) 82.

22. W.W.HUNT,Jr., and K.E.McGEE, J.Chem.Phys., 41 (1964) 2709.

23. W.W.HUNT,Jr., PB-167 193, May (1964) Air Force Cambridge Res. Lab., Bedford, Mass.

24. W.PAUL and M.RAETHER, Z.Physyk, 140 (1955) 262.

25. W.PAUL, H.P.REINHARD and U.von ZAHN, Z.Physik, 152 (1958) 143.

26. F.von BUSCH and W.PAUL, Z.Physik, 164 (1961) 581.

27. H.SOMMER, H.A.THOMAS and J.A.HIPPLE, Phys.Rev., 82 (1951)698.

28. L.FRASER MONTEIRO and R.I.REED, J.Mass Spectry.Ion Phys., 2 (1969) 265.

29. H.HURZELER, M.G.INGHRAM and J.D.MORRISON, J.Chem.Phys., 28 (1958) 76.

30. G.L.WEISSLER, J.A.R.SAMSON, M.OGAWA and G.R.COOK, J.Opt.Soc. Am., 49 (1959) 338.

31. W.A.CHUPKA, J.Chem.Phys., 30 (1959) 191.

32. J.D.MORRISON, Revs.Pure and Appl.Chem., 5 (1955) 22; J.Appl.Phys., 28 (1957) 1409.

33. H.HURZELER, M.G.INGHRAM and J.D.MORRISON, J.Chem.Phys., 27 (1957) 313.

34. H.M.ROSENSTOCK, U.S.Patent 2 999 157 (1961).

35. K.E.McCULLOH, T.E.SHARP and H.M.ROSENSTOCK, J.Chem.Phys., 42 (1965) 3501.

36. G.L.WEISSLER, "Handbuch der Physik", Springer-Verlag, Berlin, 21 (1956) 304.

37. A.TERENIN and B.POPOV, Physik.Z.Sowjetunion 2 (1932) 299.

38. F.P.LOSSING and. I.TANAKA, J.Chem.Phys., 25 (1956) 1031.

39. R.F.HERZOG and F.F.MARMO, J.Chem.Phys., 27 (1957) 1202.

40. V.E.SCHONHEIT, Z.Physik, 149 (1957) 153.

41. V.H.DIBELER and R.M.REESE, J.Res.Nat.Bur.Stand., 68a (1964)409.

COINCIDENCE TIME-OF-FLIGHT MASS SPECTROMETER

Vacuum, Inlet, Source and Tube Units

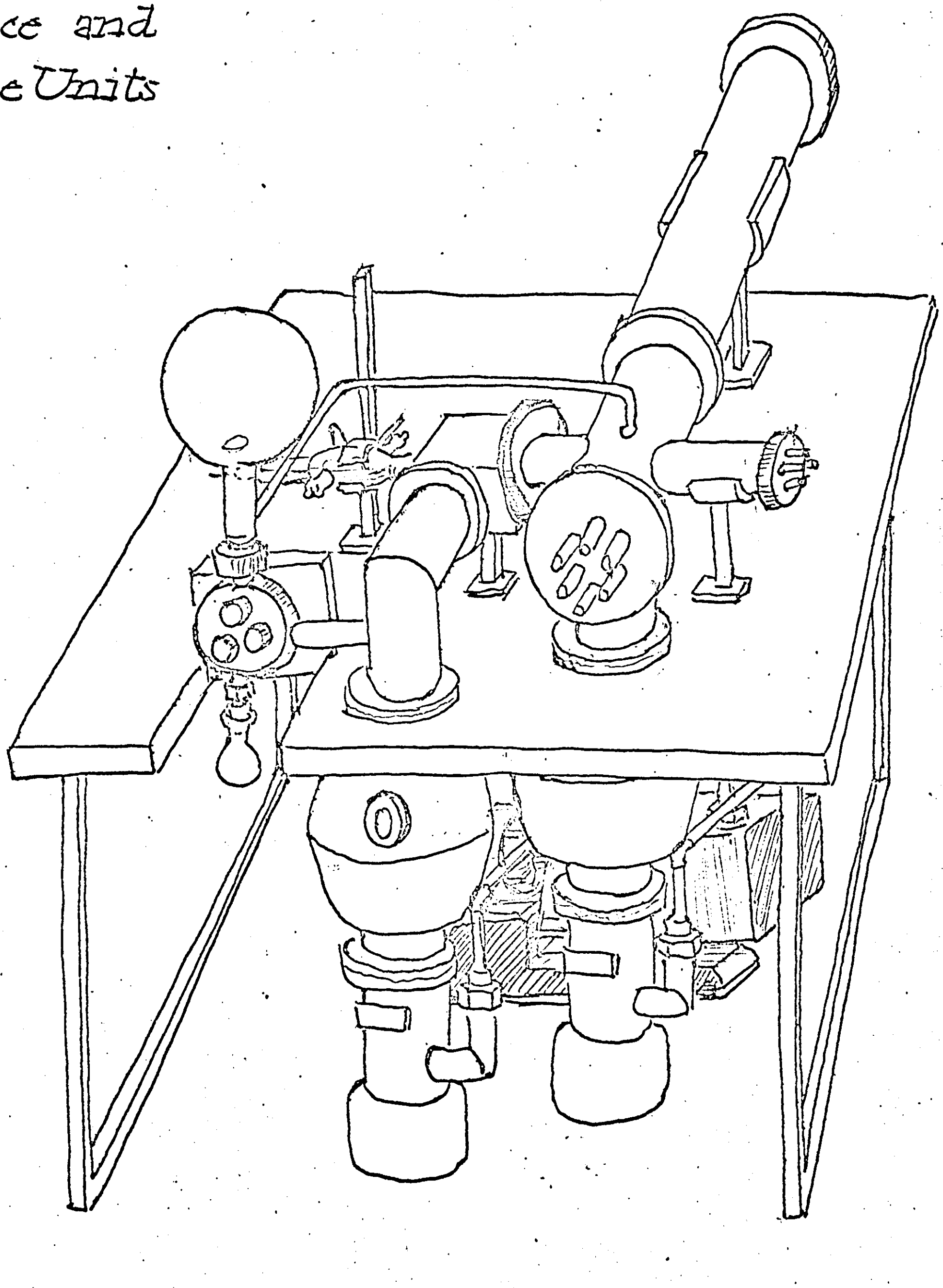

Chapter Two

DESCRIPTION
OF THE APPARATUS
AND
EXPERIMENTAL PROCEDURE

Fig. 1

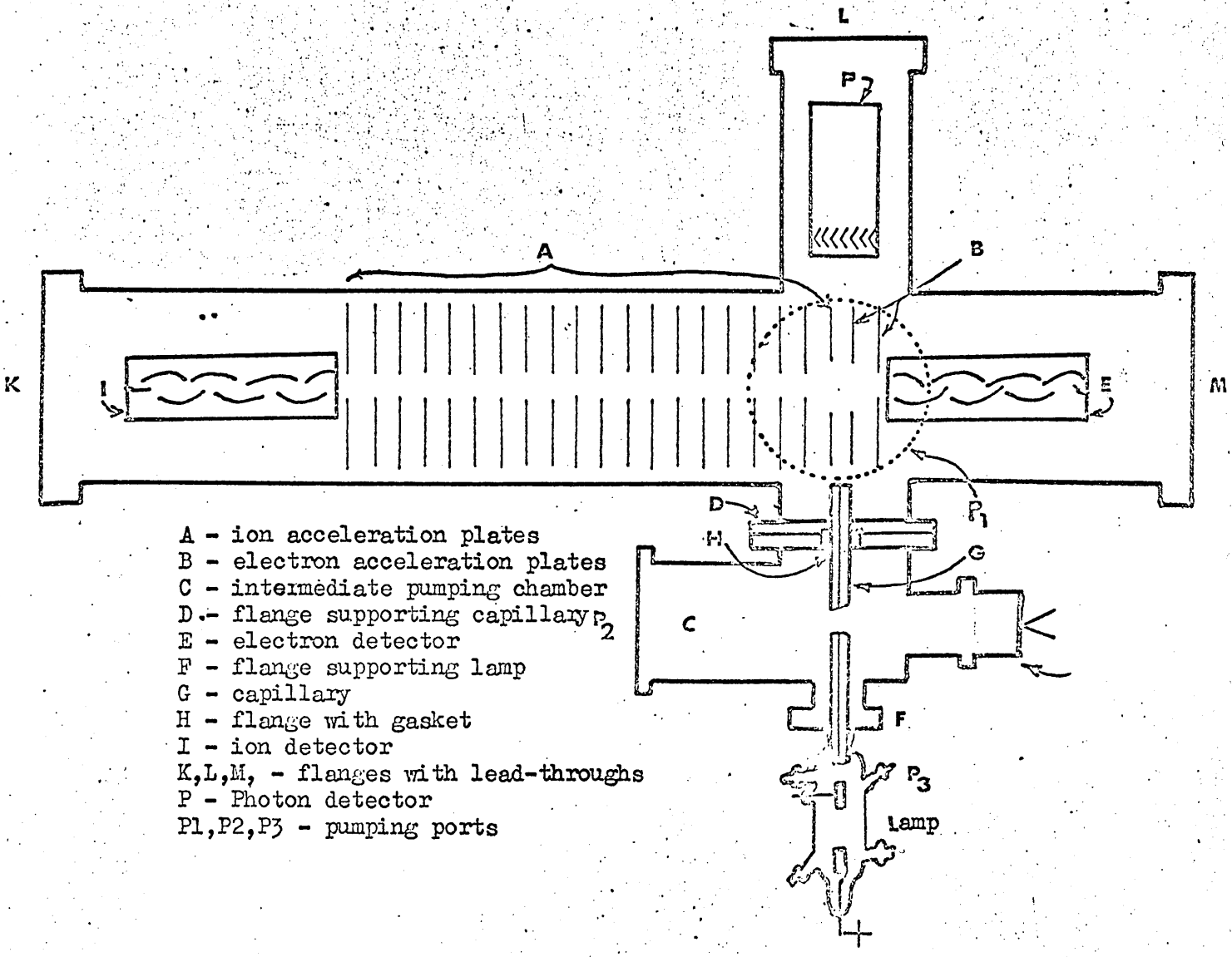

A - ion acceleration plates
B - electron acceleration plates
C - intermediate pumping chamber
D - flange supporting capillary
E - electron detector
F - flange supporting lamp
G - capillary
H - flange with gasket
I - ion detector
K,L,M, - flanges with lead-throughs
P - Photon detector
P1,P2,P3 - pumping ports

Positive ions and ejected electrons formed in a uniform electrostatic field by a photon beam of ultraviolet radiation from a helium discharge lamp are accelerated in opposite directions to multiplier detectors. The arrangement is shown in fig. 1.

The masses of the positive ions are determined by measuring the time interval between the electron and ion pulses by delayed coincidence. As the arrival of the electron to the electron detector is considered instantaneous, this difference in travel times is a measure of the ion travel time.

2.1 VACUUM SYSTEM

The housing of the spectrometer consists essentially of a cylindrical tube, 8 cm diameter and 80 cm long, with

2 side tubes 5 cm diameter, as is shown in the diagram. They are made of non-magnetic stainless steel and all the joints are argon-arc welded *
Copper gaskets are used throughout which make the system completely bakeable.

The electrical connections to the outside of the vacuum housing are made by ceramic lead-throughs inserted in the flanges K,L and M of the main tube.

A twin rotary pump, AEI type GDR210, keeps the backing pressure for two diffusion pumps P_1 and P_2, AEI type 033C, with a pumping speed of 130 l/sec, below 10^{-3} torr.

P_1 - produces the vacuum on the main tube, and P_2 - evacuates the intermediate chamber C for differential pumping between the lamp L and the main tube.

---

* Made at the Rolls Royce Ltd. East Kilbride, Scotland by kind permission of the management.

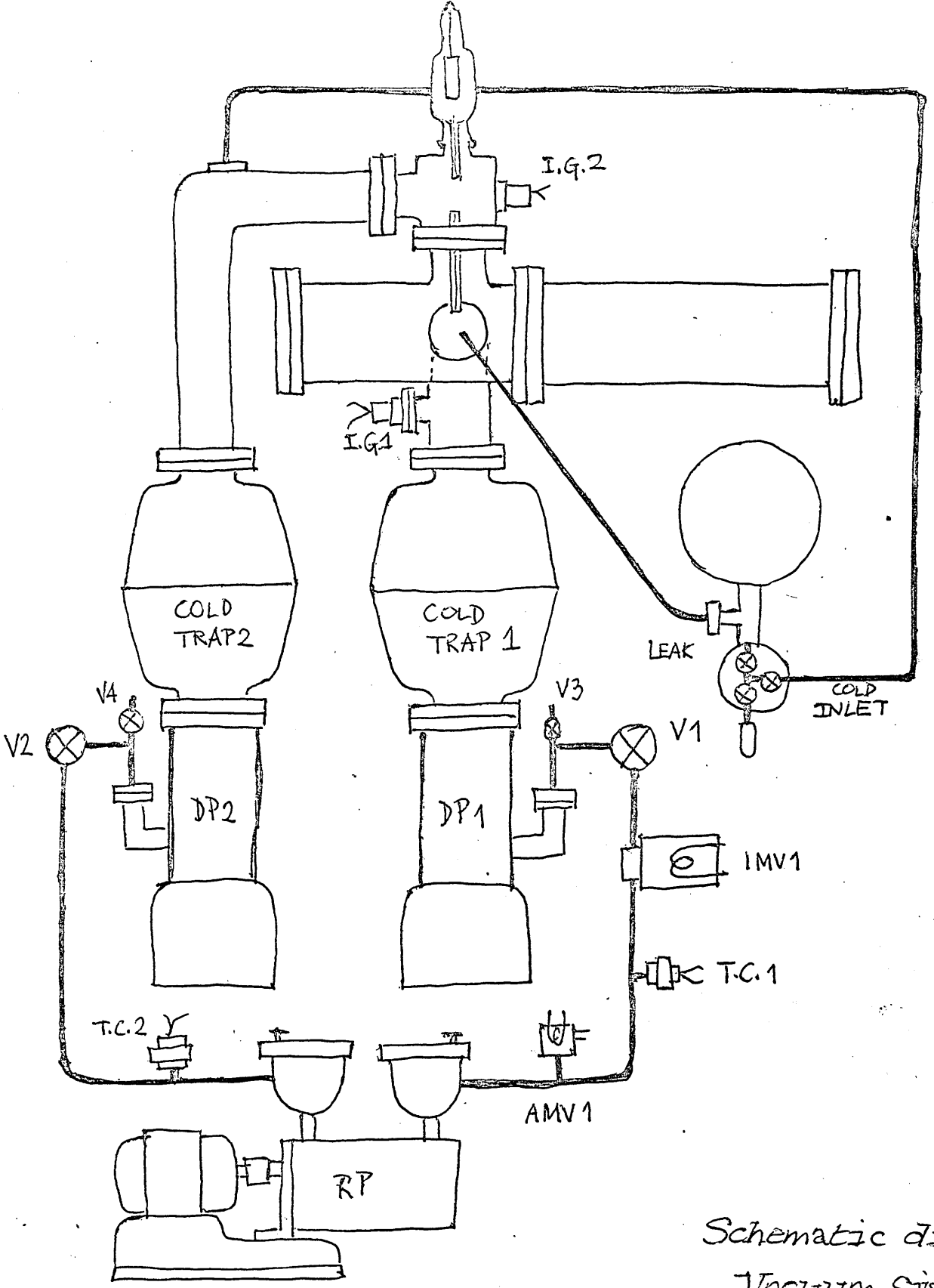

Schematic diagram
Vacuum System

Fig. 2

Both diffusion pumps are assisted by cold traps, AEI MARK III. The pressure in the backing lines of the two diffusion pumps are indicated by two thermocouple gauges, AEI type VH8, connected to the AEI VC12 thermocouple gauge control.

Magnetic valves for air admittance and simultaneous isolation of the system are used for protection against power failure.

A schematic diagram of the vacuum system is shown in fig. 2.

The path between the lamp and the ionization region is made windowless by means of a quartz capillary G through flange D that makes the connection of the chamber C with one of the lateral tubes.

The actual hole of communication between chamber C and the main tube is only the bore of the capillary G and that one can change to a capillary of different bore to allow variations on the thickness of the light beam that passes through.

This arrangement was possible due to a small flange H imbedded in flange D that makes the sealing around the capillary G.

The basic pressure in the main tube is 3×10^{-8} torr with empty cold traps, when a polyphenylether * fluid is used in the diffusion pumps.

With the helium discharge lamp in operation the basic pressure in the tube is still 3×10^{-7} torr owing to the efficient differential pumping through chamber C.

P_3 is a pumping port in the lamp L that can be connected to a rotary pump to help pumping the helium.

However, the operation of the lamp is not affected if the pumping port P_3 is closed.

The pressure measurements on the high vacuum side are made by two Bayard-Alpert ionization gauges, one below the ionization region and the second connected to the intermediate chamber C. The gauges are AEI type VH22,

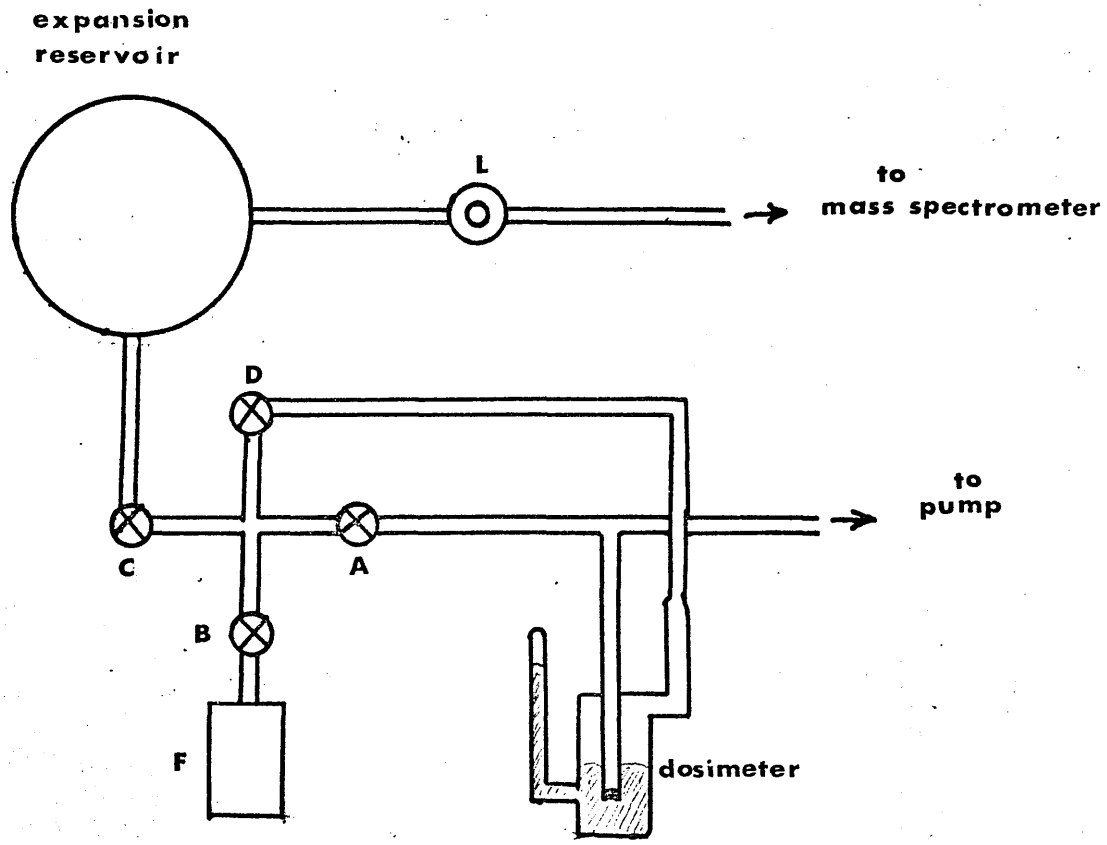
expansion
reservoir
L
to
mass spectrometer
D
to
pump
C
A
B
F
dosimeter

FIG. 3

with the control unit AEI VC20.

---

* Convalex - 10, made by Consolidated Vacuum Corporation, Rochester, N.Y., U.S.A.

2.2 INLET SYSTEM

We have chosen the batch sampling system as this one is capable of handling a wide range of sample gas volumes and pressures. In this system, small doses measured by the dosimeter are admitted to an expansion reservoir and the sample introduction for the mass spectrometer is made by a porous leak.

A schematic diagram of the inlet system is shown in fig. 3.

In this system, a common manifold of small volume is fitted with four valves, A,B,C,D.

Valve A connects the whole system to the vacuum pump P_2 which reduces the pressure in the sample system to

below 10^{-5} torr.

When valves A and C are closed, samples contained in the sample holder F are admitted via valve B to the manifold interspace, and through valve D to the dosimeter.

The dose contained in the dosimeter is admitted to the expansion reservoir, opening valves D and C. Of course, during this operation, valves B and A must be closed.

The leak valve L can then be opened and regulated for a suitable flow of the sample into the ionization region of the mass spectrometer.

The photograph on Fig. 4 shows part of the glass inlet system.

Valves A,B,C,D are vacuum tight glass taps and the leak valve L is of a special type in which a metal diaphragm seals directly on to the face of a sintered silicon carbide leak to reduce the "dead space" volume to a minimum.

This batch sampling system can be used for high vapour pressure liquids by first freezing the liquid in the

Fig.4

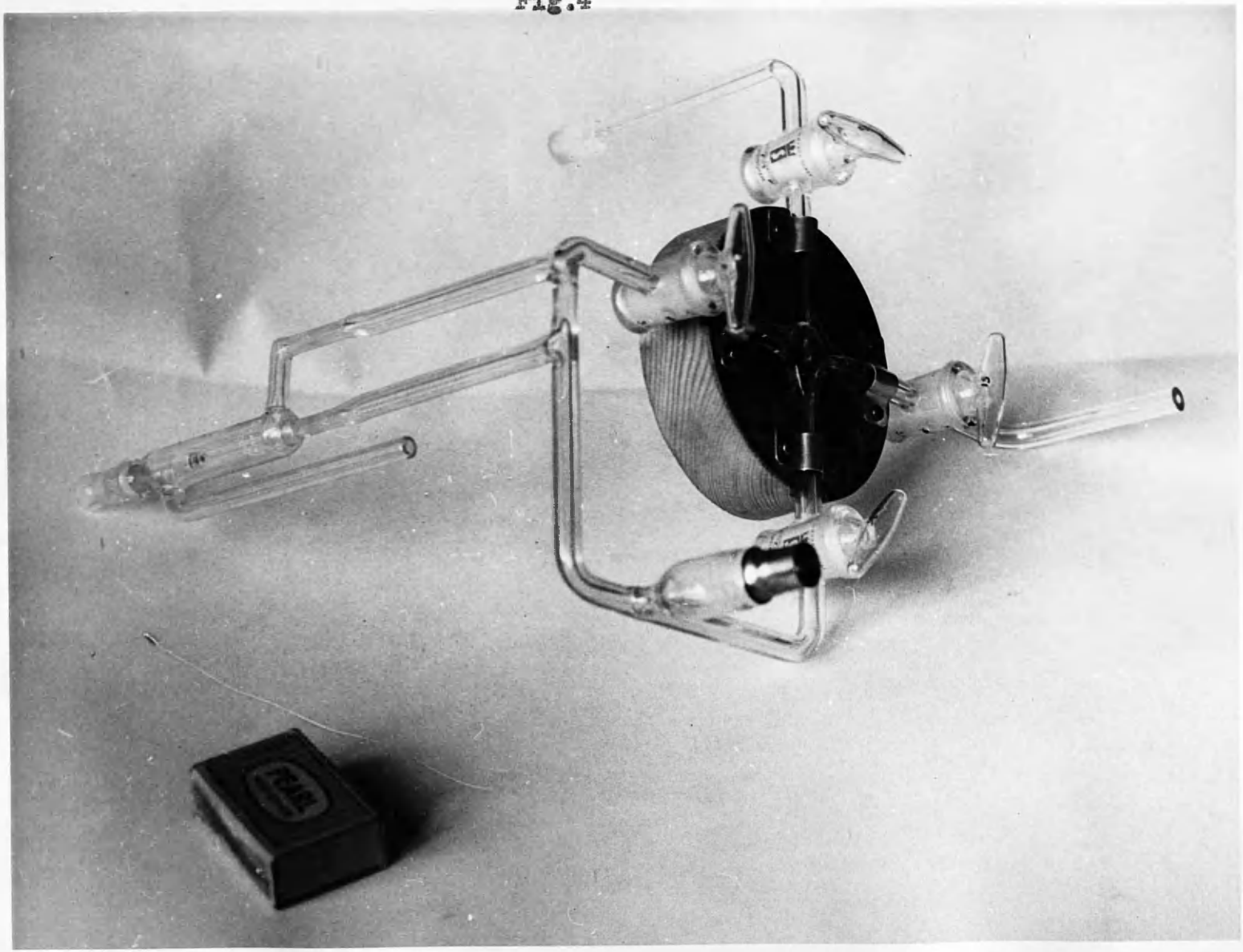

sample holder and evacuating the space above the liquid, then, by allowing the liquid to warm or, in fact, heating the liquid, introducing the vapour into the system at reduced pressure.

Because the sample pumping system consists of the rotary and diffusion pump P_2 used as well for pumping the helium through the discharge lamp, this one should not be in operation, and so the needle valve for helium admission should be closed during the pumping of the sample system to avoid sample contamination with helium.

2.3 LIGHT SOURCE

The simplest source of ultraviolet radiation is a gaseous discharge. This can be initiated by application of dc or ac potentials to the electrodes inside the gas, or by microwave radiation, or even by the radiation emitted from a Tesla coil.

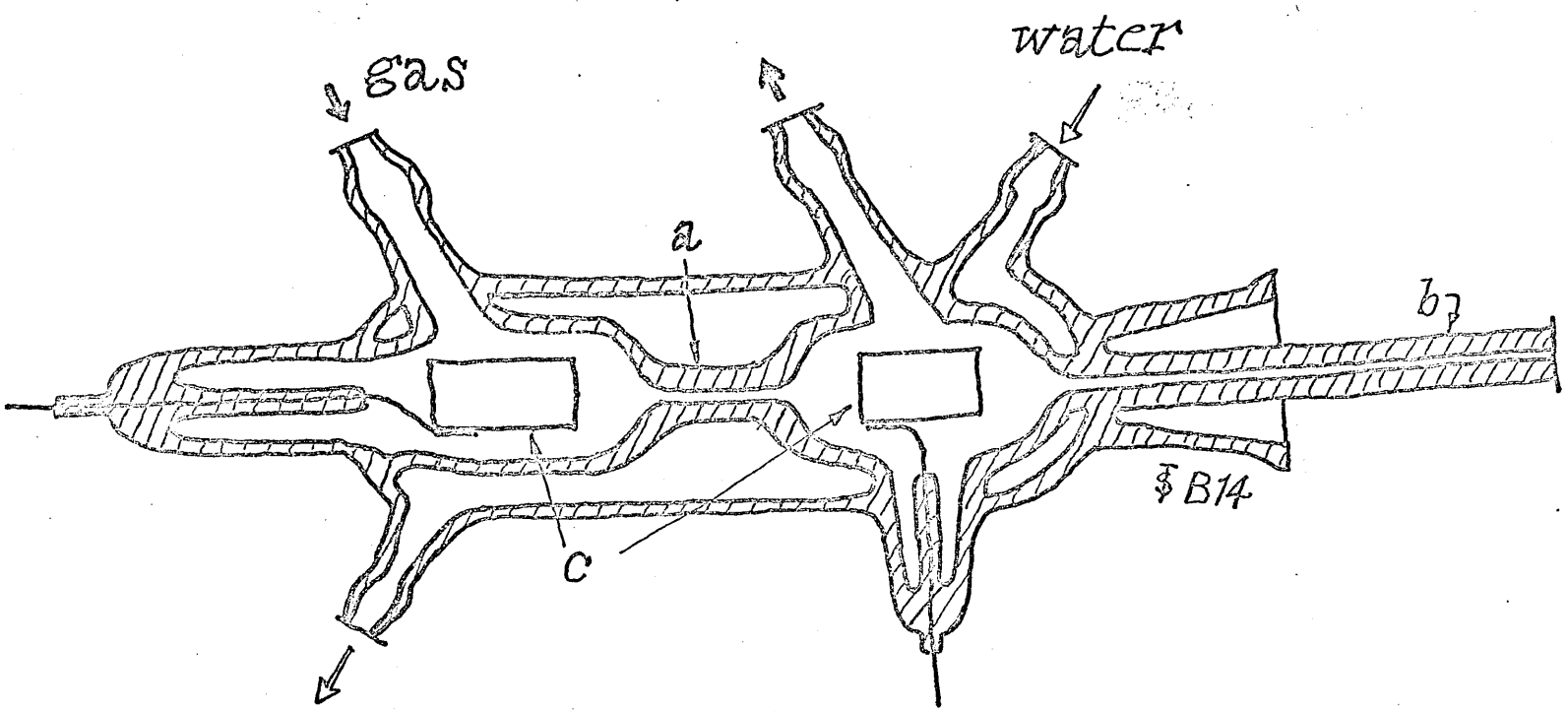

Fig.5

The light source used in our apparatus is a dc capillary discharge in helium at 1 torr pressure.

The lamp is made of Pyrex with cylindrical electrodes, made of nickel about 5 cm apart, and is water cooled.

The diagram of the lamp is shown on fig. 5.

At about 1 torr, the discharge is initiated by a voltage of around 1500 V and is maintained subsequently at about 600 V. The flow of helium from a cylinder is admitted to the lamp through a needle valve, and the first pumping port on the lamp itself is connected to a rotary pump and the remaining helium is pumped through chamber C by the diffusion P_2.

The power supply used is variable 0-2.5 KV dc stablised and regulated. The current through the lamp is about 10 mA.

The respective electronic circuits will appear in paragraph 2.6.

We believe [1,2] that the output of this lamp consists mainly of the helium emission line 584 Å (21.21ev).

As no substance is known transparent to the ultraviolet radiation of this wavelength, no window could be used between the lamp and the ionization region, which requires a high degree of differential pumping to maintain the vacuum in the analyser tube, in spite of the 1 torr pressure in the lamp.

Using a lamp with a capillary 1mm bore and the hole of communication between the intermediate chamber C and the main tube 1 mm bore also, the basic pressure in the main tube with the lamp in operation is 3×10^{-7} torr.

However, pumping through port P_3 could be eliminated without any changes in the pressure conditions if the admission of the helium was adjusted with the needle valve.

It became necessary to increase the ionization yielding and for doing that we increased the photon flux through the ionization region.

A new lamp with a 3 mm bore capillary was made and the 1 mm capillary G that makes the communication with the

ionization region was replaced by a 2 mm bore capillary. However, keeping constant the external diameter of the capillary G, no changes are necessary on flange H for the sealing.

The basic pressure in the main tube is still 8×10^{-7} torr.

The alignment of the light source with the centre of the ionization region was made through a metalic tube within chamber C with both ends fixed, one on flange D and the other on flange F.

The internal diameter of this tube was machined to fit exactly the external diameter of the capillary G and the capillary used in the light source.

There is good alighment of these capillaries in spite of the distance kept between them. The metal tube has several openings in the region between the capillaries for the diffusion of the helium into chamber C and consequent pumping.

The connection of the light source with chamber C is made on flange F with a metallic cone B14 that fits the B14 Pyrex socket of the lamp.

To keep the light source assembly stable, protected by external hazards, and also for protection of the operator from ultraviolet light, a metallic box was made to enclose the lamp. Plugs for the electrical connections, needle valve for admittance of the helium and water pipes for the cooling of the lamp, are fixed in that box.

Inside the box, and between this and the lamp, all the connections are made flexible so that the lamp can be taken out of the system and replaced very easily.

The photograph on fig. 6 shows the table top of the instrument with the assemblies described.

As it is known that the ionization yield increases when the distance between the lamp and the ionization region diminishes [3] another arrangement was studied and tested, in which only one electrode was in the lamp and the second one

Fig.6

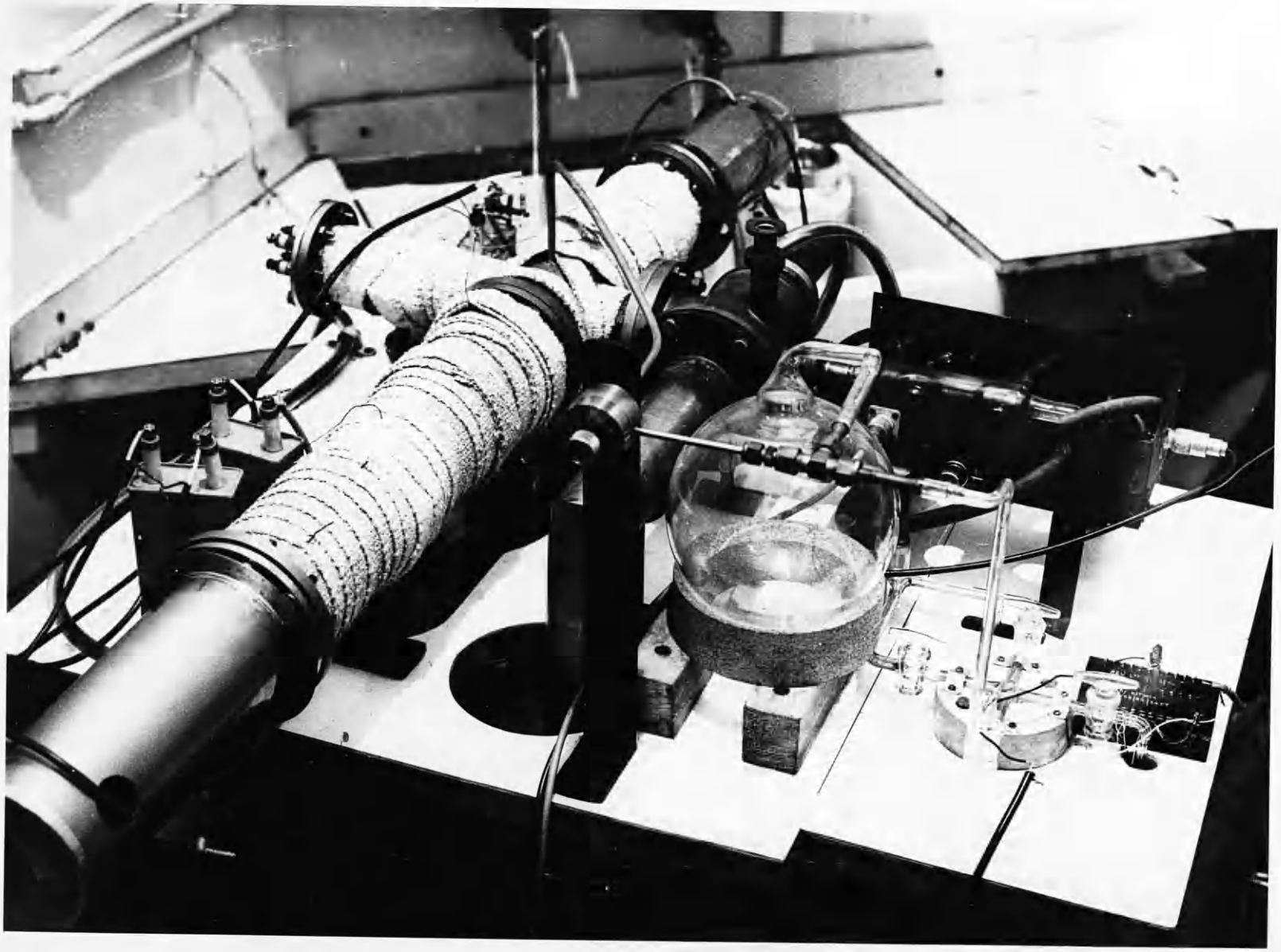

was fixed inside the chamber C.

This lamp was made of quartz and only the electrode in the lamp was water cooled.

The electrical connection for the second electrode was made by a glass to metal seal placed on chamber C.

This method proved, however, to have the disadvantage of producing the heating of the B14 cone of the lamp connection with the system, and after a certain time of operation, a leak was developed in the cone due to the melting of the apiezon wax used to make the seal between the metal cone and the quartz socket.

We tried to use Araldite for the sealing but, because the metal and quartz coefficient of expansion are quite different, after a certain time of operation the quartz socket cracked.

The problem of increasing the ionization yield was solved by increasing the photon output from the lamp with both electrodes outside the system, as already described.

2.4 PHOTON DETECTOR

The detector used for monitoring the photon intensity is an EMI photomultiplier type 95 26B, with 11 dynodes.

It was sensitised to ultraviolet radiation by coating it on the outside with a thin layer of a fluorescent solution of sodium salicylate in methyl alcohol.[4]

This coating is stable, does not evaporate in vacuum, gives reproducible results, has an excellent response, and its relative quantum efficiency is constant below 2000A°.

Because in our work we are not intended to determine photoionization efficiencies, i.e. the number of ions produced by an incident photon, we do not need an absolute calibration of the photomultiplier against a standard thermocouple,[5] or any other method for that matter.

As we have used the 584 A° helium line throughout, we only needed a recording of the anode current of the photomultiplier in arbitrary units to check if, during one experiment, the light intensity remained constant.

The light beam passes through the ionization region without striking any metal parts and impacts on the photomultiplier installed inside the vacuum system on a lateral tube opposite the photon source.

2.5 ASSEMBLY OF THE ION AND ELECTRON ACCELERATORS WITH THE RESPECTIVE ION AND ELECTRON DETECTORS.

The ion accelerator consists essentially of a set of 19 plates of non magnetic stainless steel, 0.054 cm thickness and 7.00 cm diameter. All of these plates have a circular hole in the centre of 1.0 cm diameter except for the first plate near the light beam which has a rectangular slit, 1.0 x 2.0 cm, to increase the collection efficiency of ions from the ionization region.

The electron accelerator consists of 2 plates of the same material and thickness, the plate nearest to the light beam having a rectangular slit also 1.0 x 2.0 cm and the second plate has a circular hold 1.0 cm diameter.

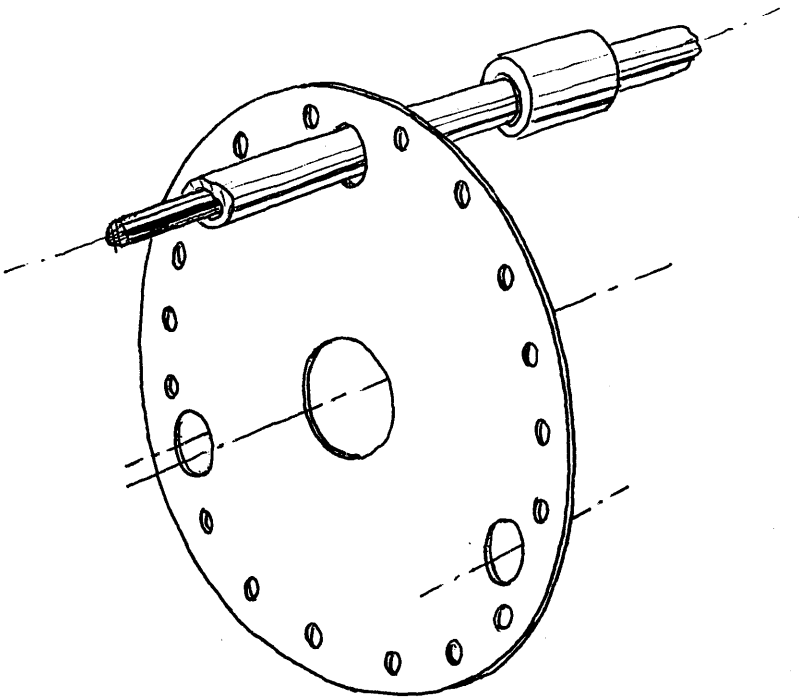

Fig.7

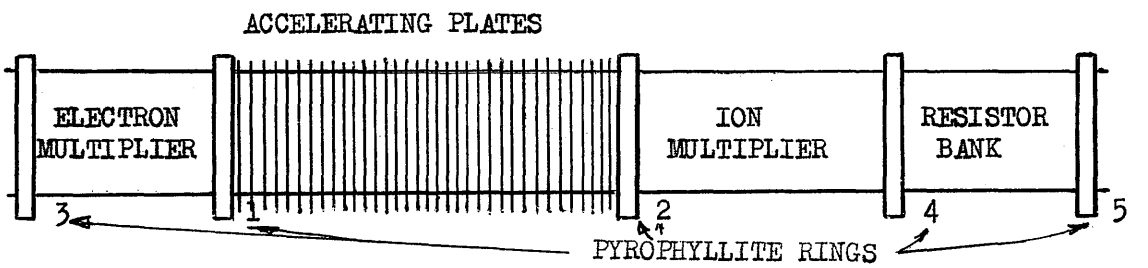
ACCELERATING PLATES
ELECTRON MULTIPLIER
ION MULTIPLIER
RESISTOR BANK
1
2
3
4
5
PYROPHYLLITE RINGS

Fig.8

All plates have a set of 3 other circular holes 0.70 cm diameter, spaced 120° on a circle of 3.0 cm radius. Three rods of 0.25 cm diameter of non magnetic stainless steel insulated by quartz tubing pass through the above mentioned holes on the plates. All plates are kept equidistant by quartz spacers 1.00 cm length, that go over the quartz tubing.

Figure 7 shows a perspective of a plate, rod, and spacer.

The three rods pass equally through 6 pyrophyllite rings machined such that the outside diameter fits exactly the internal diameter of the main tube (8 cm).

The ends of the rods are threaded to receive nuts after the rings placed in each extremity.

The assembly is shown on fig. 8.

The six rings have different shapes to accomplish the different functions they have been built to do.

This has been possible owing to the fact that

pyrophyllite is a very easily machinable ceramic and after being fired to about 1200°C assumes the desired insulator properties with practically no porosity [6].

Rings 1 and 2 have appropriate grooves to suit the glass envelopes of ion and electron multipliers respectively that have been cut about 0.5 cm from the first dynode.

Ring 3 was machined to fit the base of the electron multiplier.

Rings 4 and 5 have been designed to receive the bank of resistors in series that supplies the potential gradient to the ion accelerator. The resistors are connected with stainless steel connectors between the metal pins through 2 pinched glass bases supported by rings 4 and 5.

Ring 4 has a special shape for, besides the function of keeping the pinched glass base, it centres the ion multiplier and makes the electrical connections of each resistor with each plate by means of stainless steel connectors housed in circular holes on the periphery of

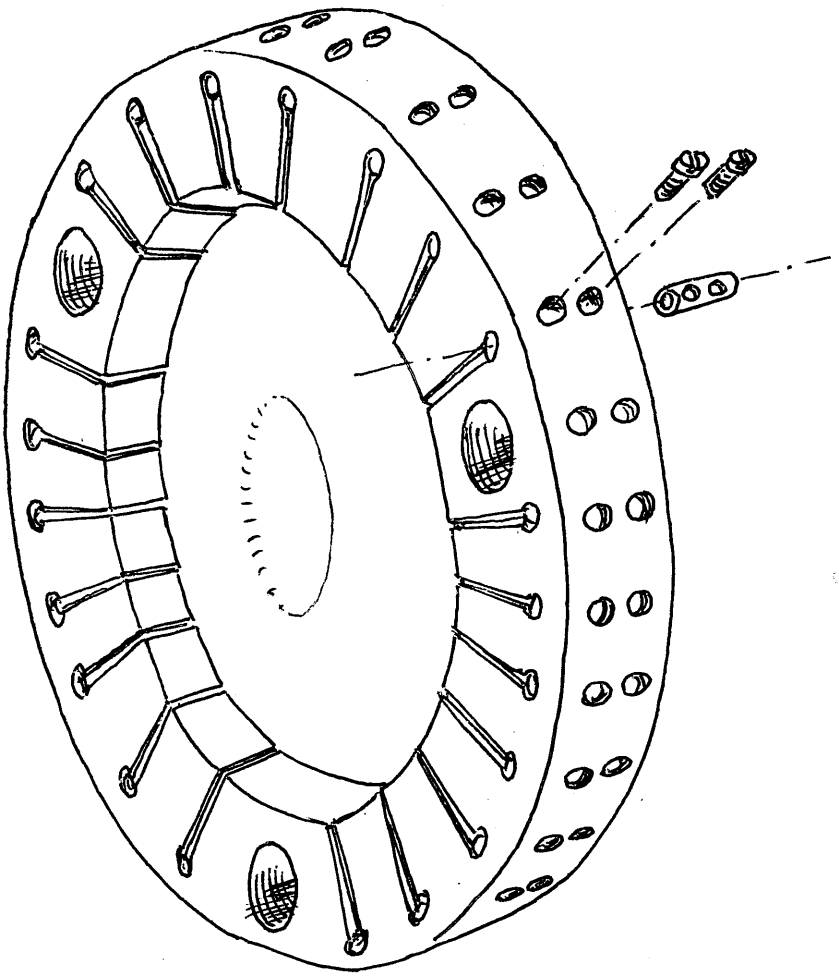

Fig.9

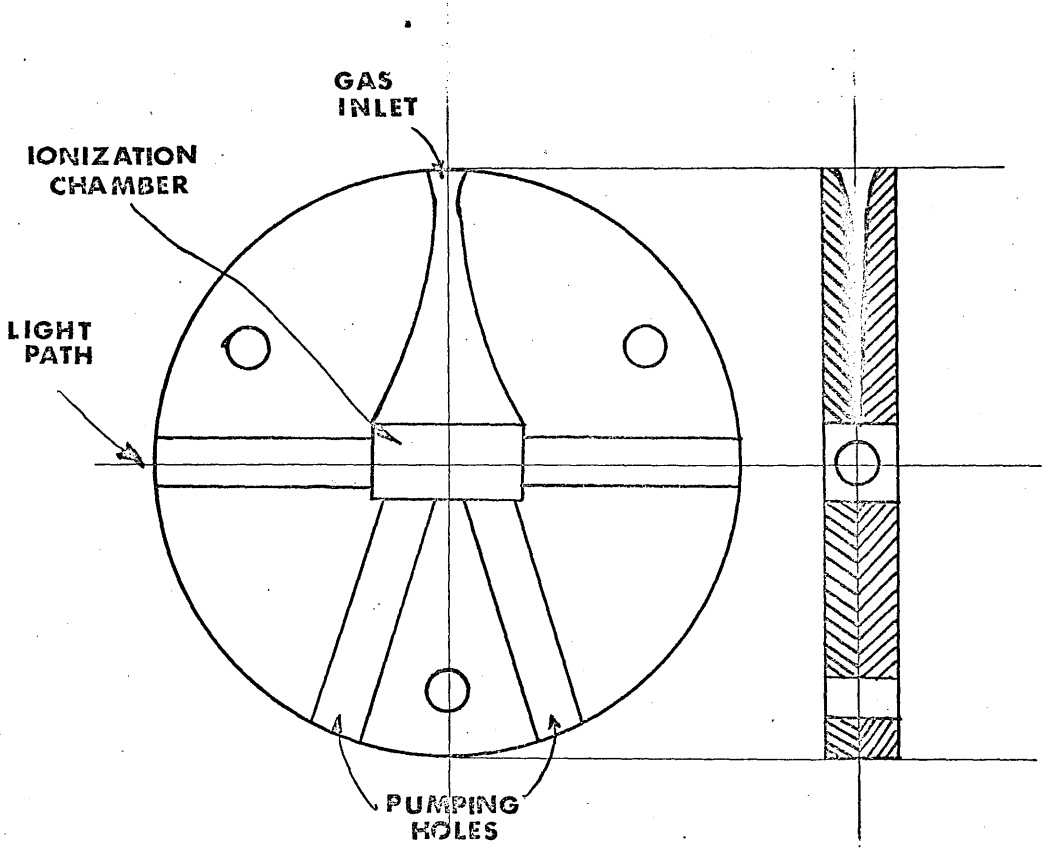

Fig. 10

the ring. Nickel wire insulated by quartz sleeving passing through circular holes made on the periphery of the stainless steel plates makes the connection between the plates and each connector.

A schematic diagram of ring 4 is shown in fig. 9.

Ring 6 was introduced at a later stage on the ionization region between the two plates with rectangular slits to diminish the ionization region volume and so increase the concentration of sample molecules in this region.

Fig. 10 shows a schematic diagram of Ring 6.

The majority of sample molecules from the inlet system are forced to go into the circular hole on the pyrophyllite ring owing to the fit contact of the ring with the tube walls, and after passing across the light beam, the neutral molecules are pumped through two holes provided.

The light beam passes through a circular hole on the

ring and is horizontal and transverse with respect to the electrostatic field created by the set of plates.

With this arrangement, the assembly with accelerator plates and detectors makes a single unit that can be put in and out the tube as a whole.

There is, therefore, access to every piece within the tube for eventual replacement or modifications, as, for example, to increase or diminish the number of plates either on ion or electron side.

Fig. 11 shows a photograph of the whole assembly inside the main tube.

All the pieces, plates and rings, have been made in our workshop.

Great care was observed to have the plates perfectly plain and the central hole absolutely circular. The plates surfaces were polished to a very smooth finish.

These details are absolutely essential to ensure that the electrical field through the plates is uniform.

Fig.11

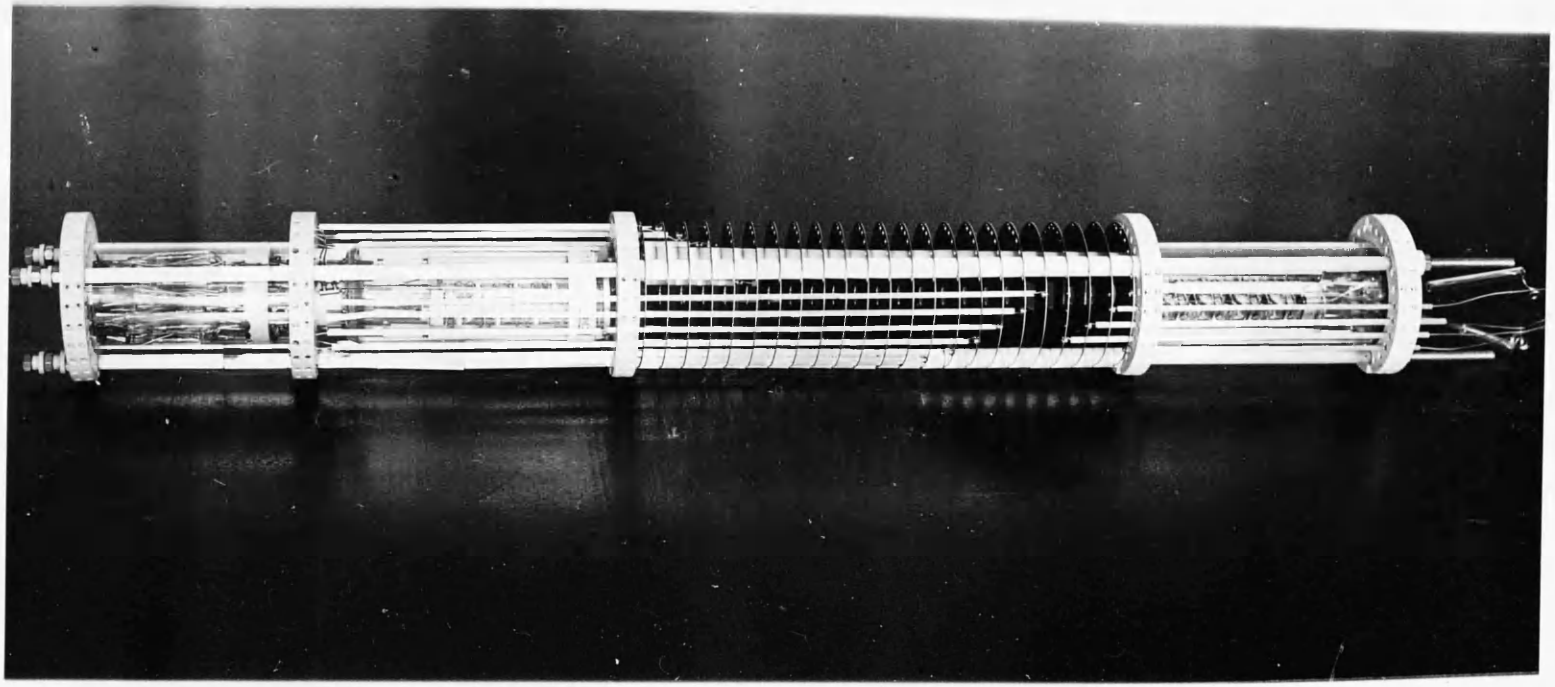

The quartz spacers * were within the tolerance of 1.00 $\pm$ 0.05 cm.

The resistors used in the potential divider are low noise, 2% tolerance 11 MΩ value.

The alignment of the light beam on the centre of the ionization region is made by the lateral tube opposite the light source and care was taken to avoid the light striking any metal or pyrophyllite pieces.

The rectangular slits on the pyrophyllite ring and plates, one on each side of the ring, with the major dimension 2.0 cm horizontal and parallel to the light beam, limit the region from which ions and electrons can be collected.

The electron detector is an EMI box and grid multiplier type 9707 with 17 beryllium-copper dynodes in which glass encapsulated and bakeable resistors for the dynode chain are already incorporated.

The beryllium-copper surfaces give a detection

efficiency of 90-100% to a single electrons of energy 300 - 500 eV, falling to 50% as the incident energy increases to 2.5 KeV. For energies between 2.5-5 KeV, the efficiency remains substantially constant at 50%.

* Supplied by Thermal Syndicate Limited, Wallsend, England.

The nominal gain of the electron multiplier was at 2 KV bigger than 10^5, but after the dynodes have been exposed to air for several periods, the gain dropped considerably. However, the gain and signal to noise ratio have improved [7] by baking the multiplier at 300°C in oxygen at atmospheric pressure during one hour.

The ion detector is an EMI beryllium-copper venetian blind dynode system type 9642 with 18 dynodes and the nominal gain of bigger that 10^6 at 3KV. This multiplier was supplied with the glass incapsulated and bakeable resistors for the dynode chain also.

The ion detection efficiency varies with impact

VARIATION OF DETECTION EFFICIENCY OF THE PARTICLE MULTIPLIER (TYPE 9603) WITH ION IMPACT ENERGY

(TYPE 9642 GIVES 40 X GAIN OF TYPE 9603)

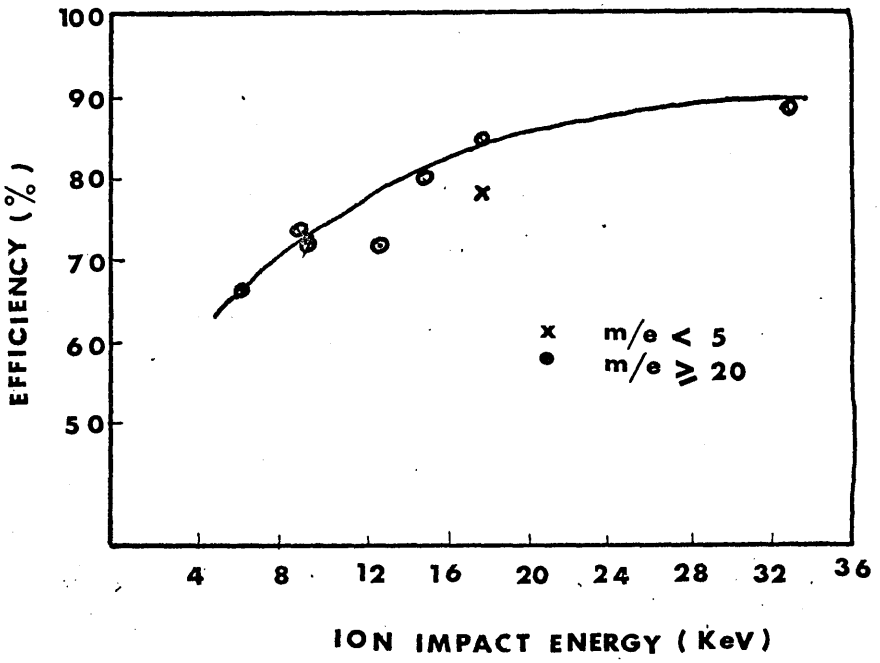

FIG. 12

energy for a beryllium-copper multiplier in the way shown on the curve in fig. 12.[8]

Efficiencies of better than 85% are obtained for ions of impact energy 18 KeV, and better than 60% for 6 KeV. The efficiency is not greatly affected by ion-mass but is slightly greater for heavier ions. This contrasts sharply with the behaviour of ionization chambers, solid state detectors and scintillation counters.

Beryllium-copper multipliers are insensitive to wavelengths in the visible region, having their threshold at about 2900-3000 Å.

Little is known of the quantum efficiency of this material but is thought to peak at a value of about 20% at 700 Å. This value is very approximate.

Over the soft X-ray region it is about 1-5%; at 200 Å it is about 0.1% and 0.2% for X-rays of wavelength 4.74×10^{-3} Å.

The Kodial envelope in both multipliers was shielded

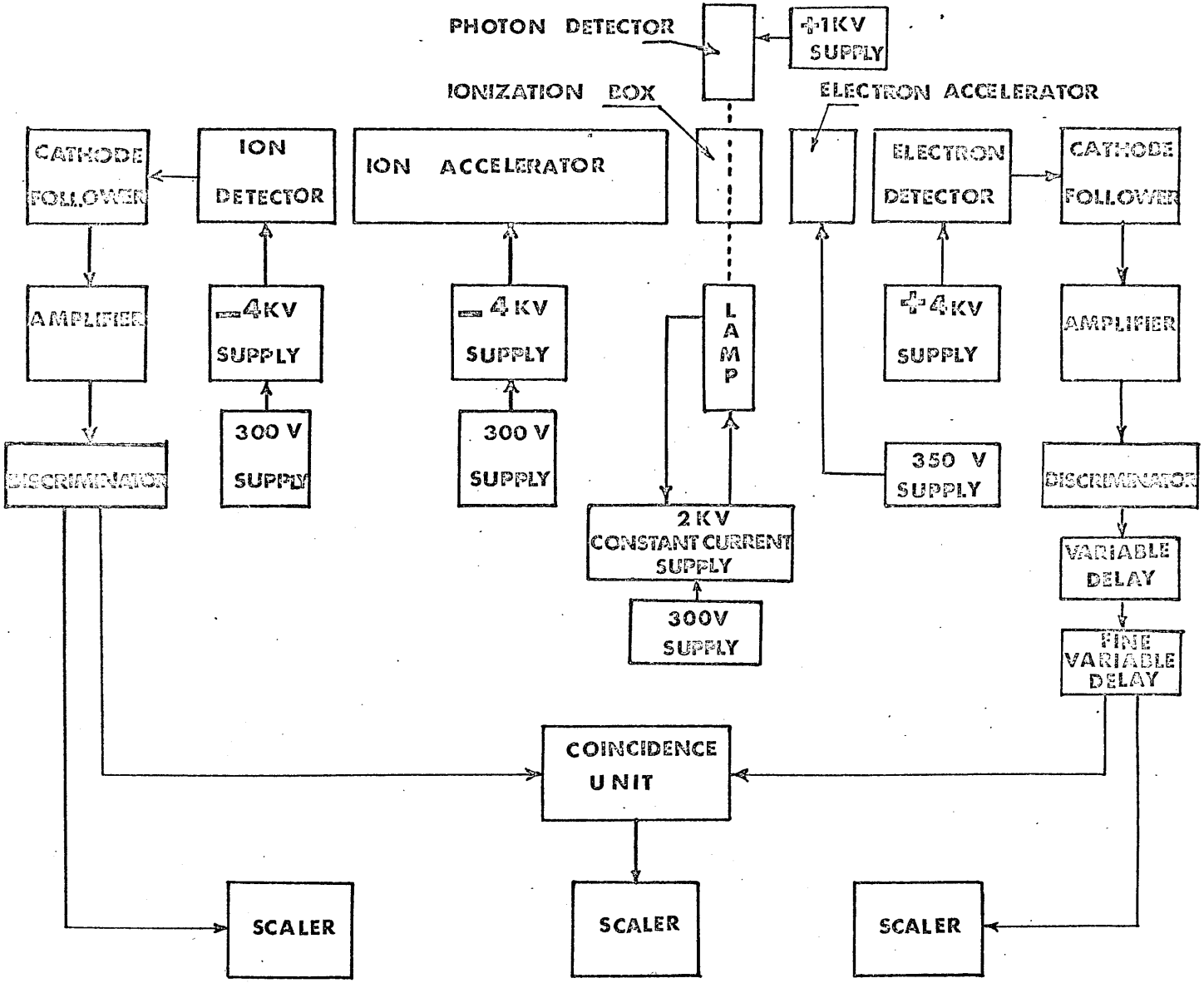
PHOTON DETECTOR
+1KV SUPPLY
IONIZATION BOX
ELECTRON ACCELERATOR
CATHODE FOLLOWER
ION DETECTOR
ION ACCELERATOR
ELECTRON DETECTOR
CATHODE FOLLOWER
AMPLIFIER
−4KV SUPPLY
−4 KV SUPPLY
LAMP
+4KV SUPPLY
AMPLIFIER
300 V SUPPLY
300 V SUPPLY
350 V SUPPLY
DISCRIMINATOR
DISCRIMINATOR
2 KV CONSTANT CURRENT SUPPLY
VARIABLE DELAY
300V SUPPLY
FINE VARIABLE DELAY
COINCIDENCE UNIT
SCALER
SCALER
SCALER

Fig 13

by Co-Netic magnetic foil [9] grounded to eliminate environmental electric and magnetic fields.

The interior of the main tube was also lined with the magnetic shielding to protect all the space occupied by the plates from external fields.

2.6 ELECTRONIC UNITS AND CIRCUITRY

The layout of all electronic units involved is shown in fig. 13.

After a neutral molecule is ionized, the resulting positive ion and electron are accelerated in opposite directions by the appropriate fields.

Ejected electrons from the ionized molecules fall through a potential gradient of 350 V and impact on the first dynode of the electron multiplier that is also kept at 350 V positive.

Ions are accelerated in opposite directions by the electrostatic field which is uniform in direction and

strength (200 V/cm), created by the set of plates and impact on the first dynode of the ion multiplier held at about - 3000V.

Only in the final few centimetres of the ions' travel there is field penetration from the first dynode of the multiplier but this has minor effects on paths and travel times.

The electron path is very short (about 2 cm) and, due to the very small mass of the electron, the travel time to the electron collector is negligible (about 5 nsec) in comparison with the longer travel times of the ions in opposite directions.

Pulses of short duration - about 20 nsec - are received from the anodes of both multipliers.

The electron pulses are about 1-2 mV amplitude and the ion pulses are between 5-15 mV due to the higher gain of the ion multiplier.

The pulses from the two multipliers are fed to

separate cathode followers and are amplified in separate amplifiers and shaped by amplitude discriminators.

The resulting ion pulse is presented to the first channel of a coincidence unit.

After discrimination, the electron pulse is delayed in a variable delay network to cover the time of flight of the particular ion-mass we are interested in.

The output from the delay is fed to a second channel on the coincidence unit.

If the delay set on the delay line is of appropriate value, both ion and the electron pulses should arrive at the coincidence unit at the same time, within limits set by the pulse width.

Single channel pulses are rejected by the coincidence unit and only the coincident pulses give rise to output pulses from the coincidence unit to be counted on a scaler.

In practice, a mass spectrum is recorded by varying the delay time on the delay line against the number of

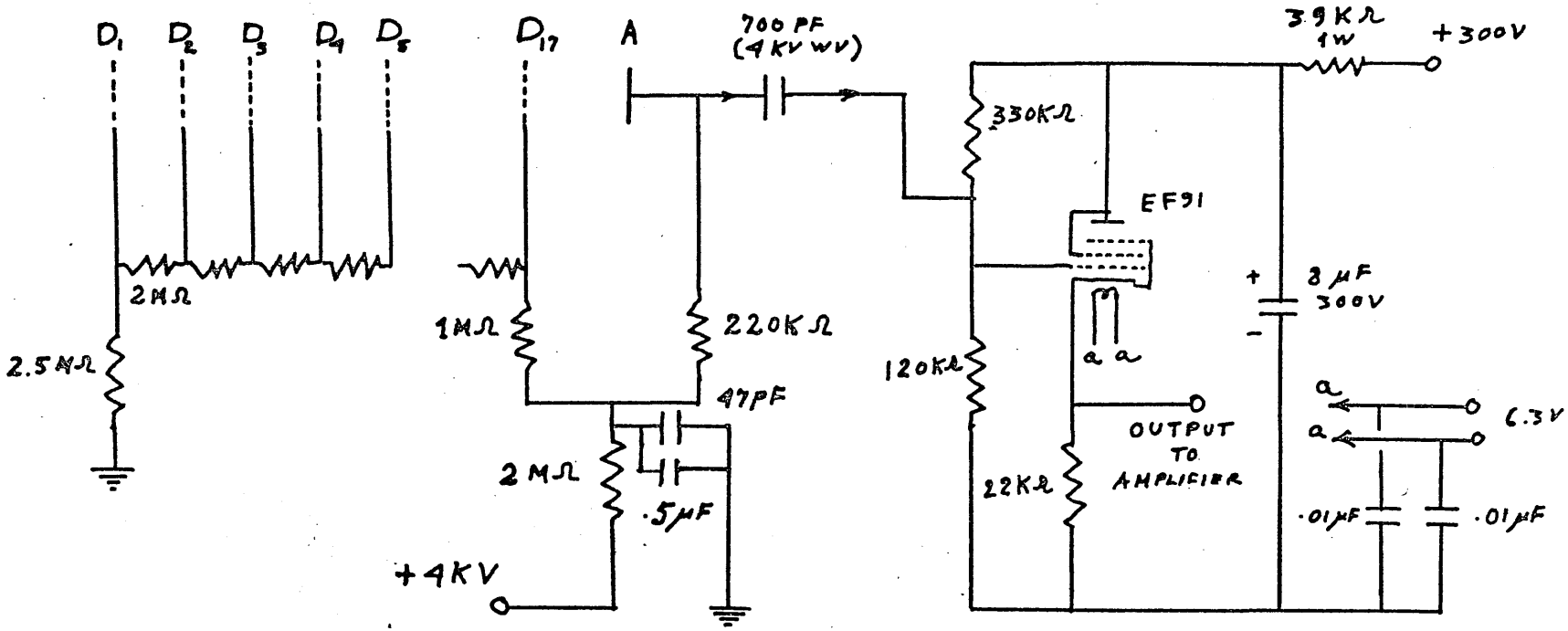
D1
D2
D3
D4
D5
2MΩ
2.5MΩ
D17
A
700 PF
(4 KV WV)
1MΩ
220KΩ
47PF
2 MΩ
.5μF
+4KV
330KΩ
3.9KΩ
1W
+300V
EF91
8 μF
300V
120KΩ
22KΩ
OUTPUT
TO
AMPLIFIER
6.3V
.01μF
.01μF

Fig. 14

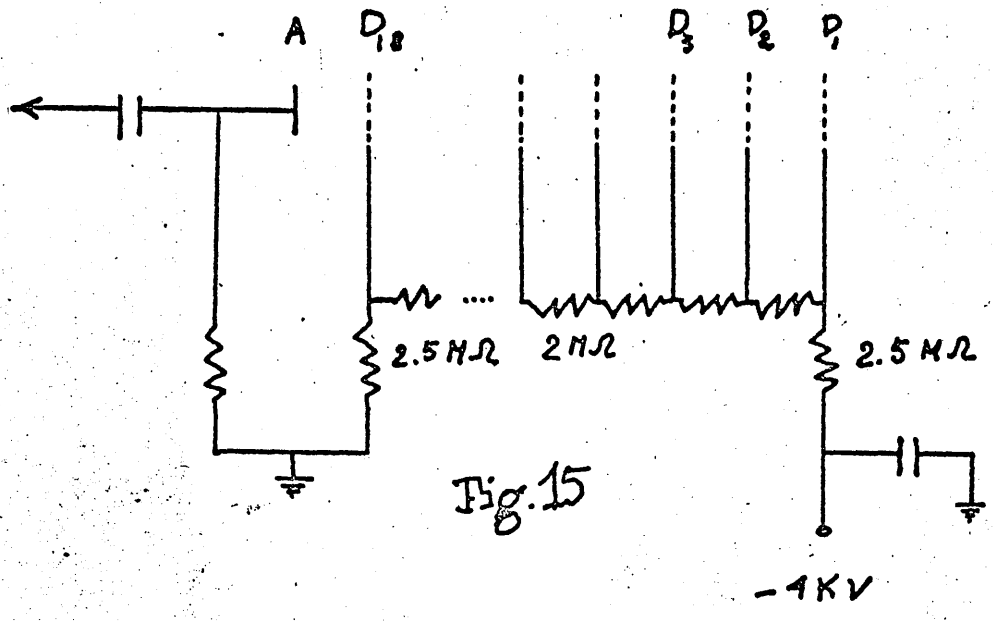

Fig. 15

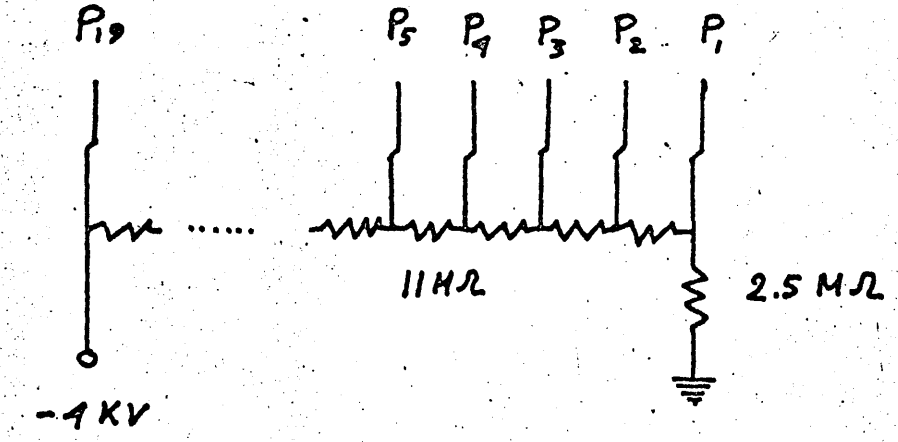

Fig. 16

counts registered on the scaler.

Ion mass measurement is based on the fact that the delay required to a certain ion species is a linear function of the square root of the mass-to-charge ratio for that species.

The electrical connections on the electron multiplier are as in fig. 14. The 300 V positive and 6.3 V for the heaters on the cathode follower are supplied by the Amplifier (I.D.L. wide-band type 652). The cathode follower is outside the vacuum but very near the anode of the multiplier. On the ion multiplier side the connections are shown in fig. 15 and those for the ion acceleration plates are shown in fig. 16.

The first plate is slightly below ground and the last is at high negative potential. We normally use the last plate at about - 2000 V, which brings the first plate to a potential about 50V below ground, but these values are variable.

In fact, the scanning of the mass spectrum could be done, keeping the delay of the electron pulse constant and varying the field on the ion accelerator plates.

However, we found this method not completely satisfactory because when the potential on the first plate changes and so the potential gradient across the ionization region, the focusing properties of the plates are changed and the ion collection efficiency varies accordingly.

Also, the variation in the efficiency of ion multiplier with the energy of the incident ions- as shown graphically in p. 2.5 - militates against this form of scanning.

In our apparatus, we found that varying the ion acceleration from 2000 V to 2800 V, the number of ions detected by the multiplier without coincidence varies from 1200 to 1600 per minute, in one instance.

Because of this, we kept the acceleration voltage constant and the scanning was done on the delay line.

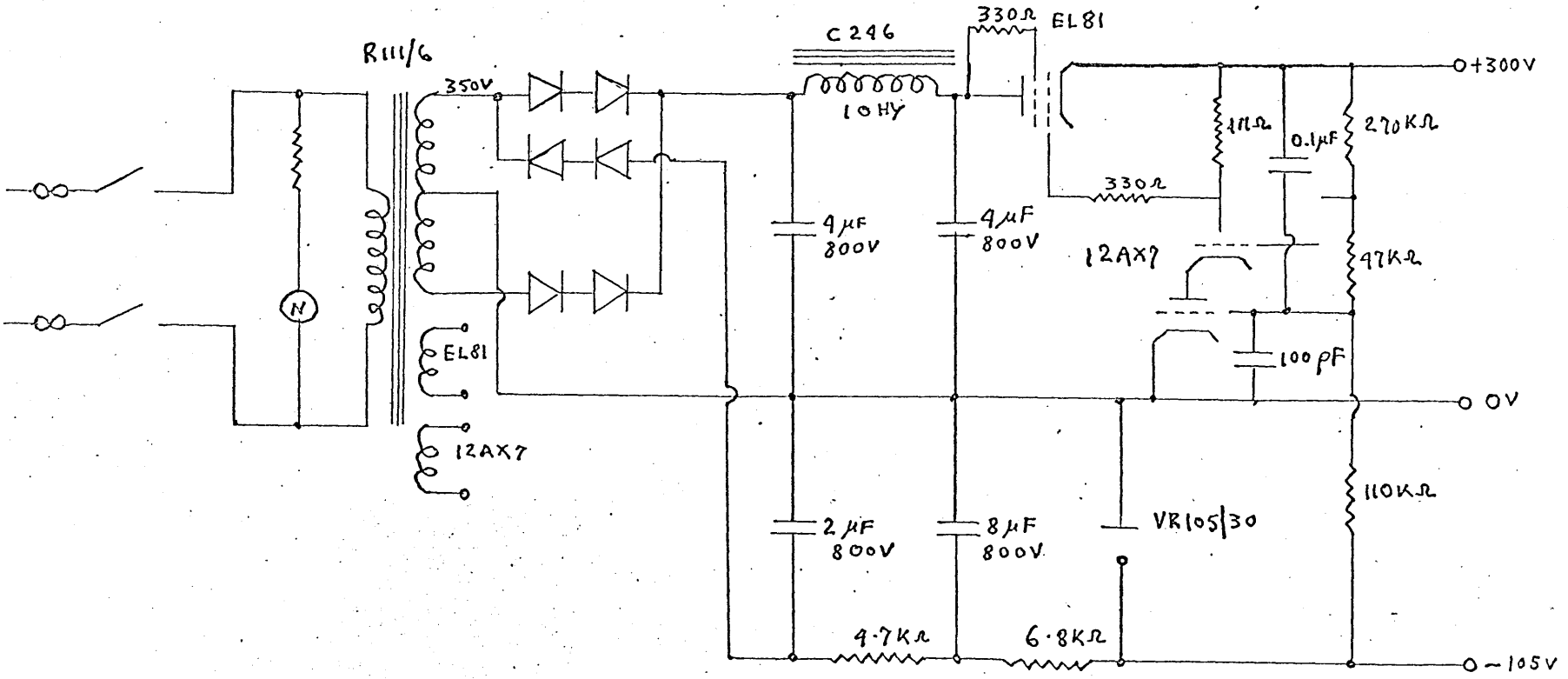
R111/6
350V
N
EL81
12AX7
C246
10 HY
330Ω
EL81
4μF
800V
4μF
800V
330Ω
1MΩ
0.1μF
270KΩ
12AX7
47KΩ
100pF
+300V
0V
110KΩ
2μF
800V
8μF
800V
VR105/30
4·7KΩ
6·8KΩ
−105V

Fig. 17(a)

Care was taken to reduce to a minimum all sources of noise or ripple.

The electronic circuits used for the 4 KV supplies are modifications of the EKCO E.H.T. supply and the respective circuitry is shown on fig. 17.

The noise and ripple of these supplies is less than 15 mV r.m.s. The stability is 0.5 V between no-load and full-load operation. The circuitry for the power supplies to the light source is shown in fig. 18.

The grounding of all electronic apparatus involved, where 50 cycle pick-up was troublesome, appeared to be more of an art than a science.

It was specially difficult when combined with earthing for safety.

There seems to be nothing better than trial and error [10].

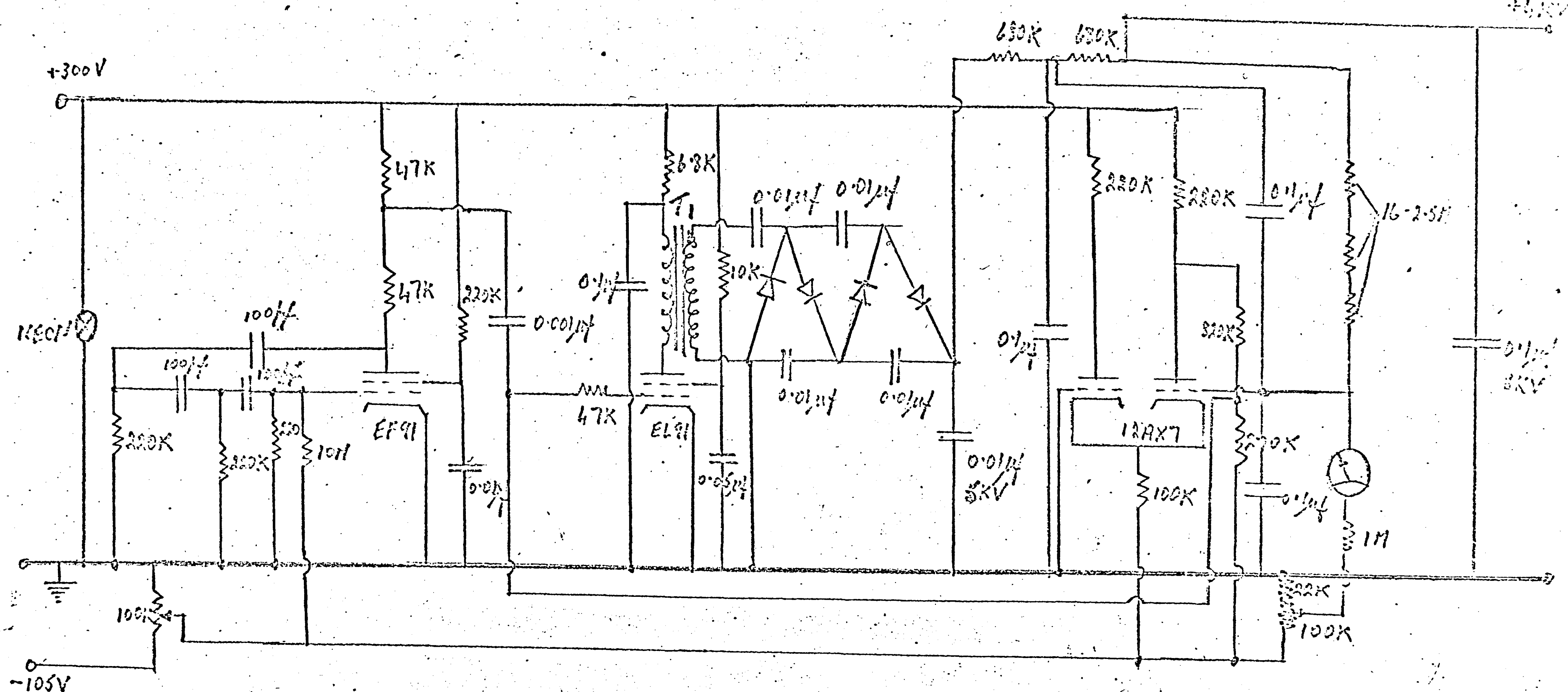
+300V
NEON
100pf
220K
47K
EF91
0.01μf
6.8K
T1
0.1μf
EL91
10K
0.01μf
0.05μf
5KV
680K
+4KV
12AX7
100K
16-2.5M
1M
22K
-105V

Fig. 17(b)

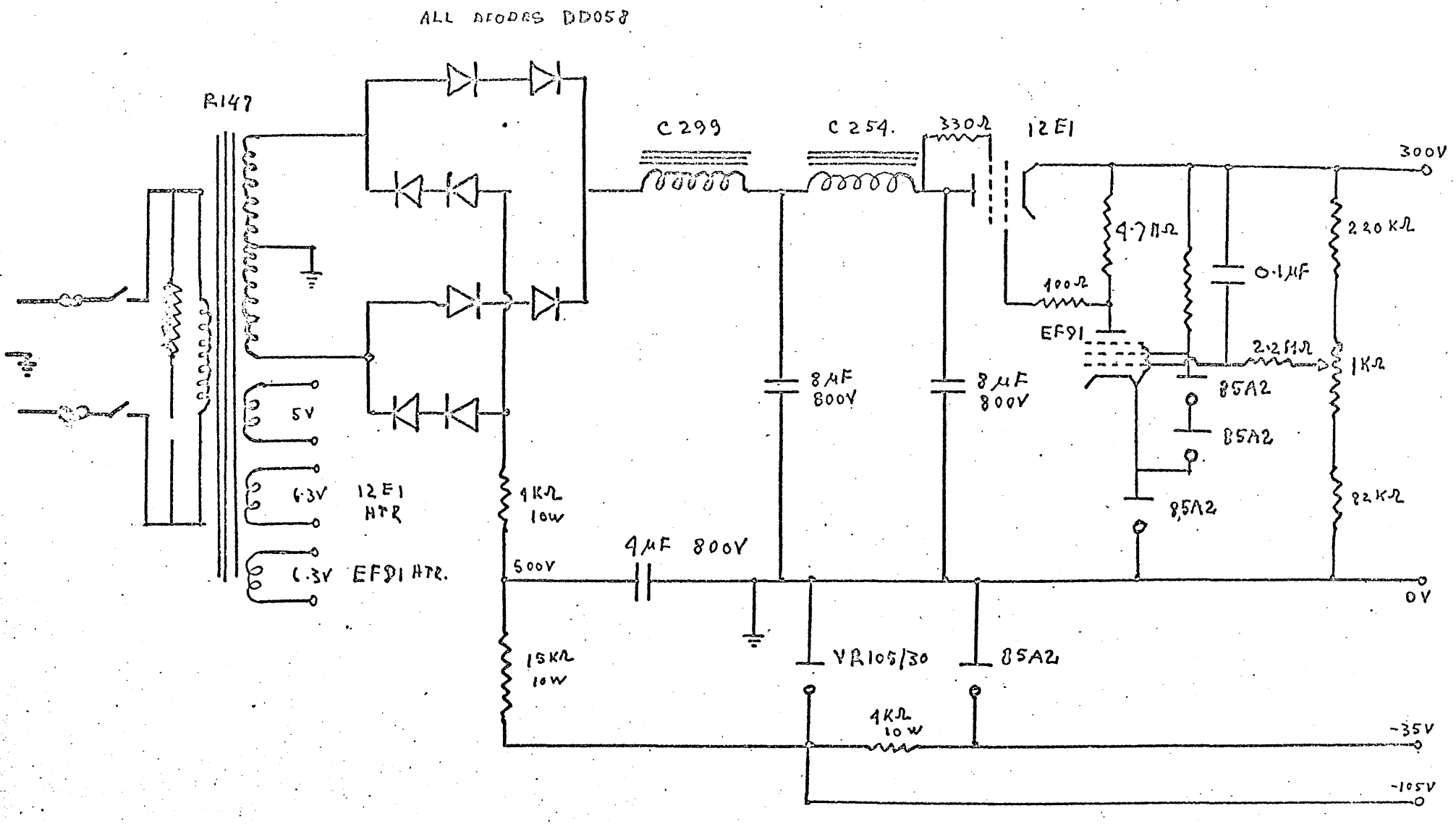
ALL DIODES DD058
R147
C299
C254.
330Ω
12E1
300V
4·7MΩ
220KΩ
0·1μF
100Ω
EF91
2·2MΩ
1KΩ
85A2
85A2
85A2
8,5A2
82KΩ
8μF 800V
8μF 800V
5V
6·3V 12E1 HTR
6·3V EF91 HTR.
4KΩ 10W
4μF 800V
500V
0V
15KΩ 10W
VR105/30
85A2
4KΩ 10W
-35V
-105V

Fig. 18(a)

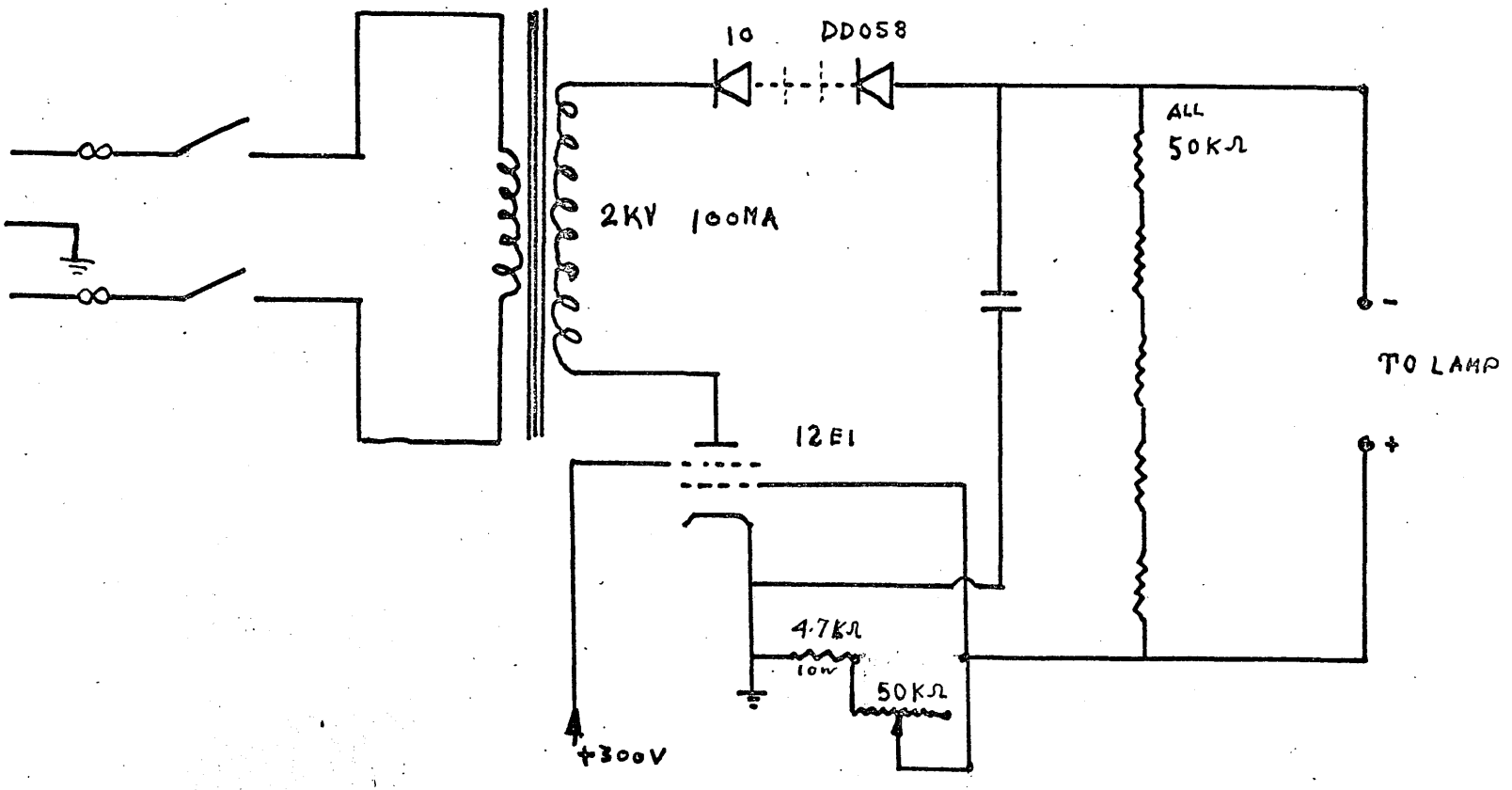

Fig. 18(b)

REFERENCES

1. J.H.BEYNON, A.E.FONTAINE, D.W.TURNER and A.E.WILLIAMS, J.Sci.Instr., 44 (1967) 283.
2. D.C.FROST, C.A.McDOWELL, J.S.SANDHU and D.A.VROOM, "Advan.Mass Spectry.", 4, Institute of Petroleum, London (1968) 781.
3. J.H.BEYNON, A.E.FONTAINE, D.W.TURNER and A.E.WILLIAMS, J.Sci.Instr., 44 (1967) 283.
4. F.S.JOHNSON, K.WATANABE and R.TOUSEY, J.Opt.Soc.Am., 41(1951) 702.
5. N.WAINFAN, W.C.WALKER and G.L.WEISSLER, J.Appl.Phys., 24(1953)1318.
6. Information made available by V.G. PORCELAIN Co.LTD., Gorst Rd., Park Royal, London N.W.10.
7. J.R.YOUNG, Rev.Sci.Instr., 37 (1966) 1414 (Eng).
8. E.M.I., Brochure ref.30M/6-67 (PMT).
9. MAGNETIC SHIELD DIV., PERFECTION MICA CO., Chicago, Ill.
10. E.BRIGHT WILSON, "An Introduction to Scientific Research" McGraw--Hill, New York,(1952) 112.

Chapter Three

THEORETICAL CONSIDERATIONS

3.1. PHOTOIONIZATION PROCESSES

Consider a molecule R_1R_2 in which R_1 and R_2 are two atoms or radicals covalently bound; three photoionization processes can occur:

(1a) Ionization to the ground state of the ion

$$R_1R_2 + h\nu \rightarrow R_1R_2^+ + e^-$$

(1.b) Ionization to an excited state of the ion

$$R_1R_2 + h\nu \rightarrow R_1R_2^{+*} + e^-$$

(2.a) Fragmentation of the parent ion

$$R_1R_2 + h\nu \rightarrow R_1R_2^+ + e^-$$
$$\downarrow$$
$$R_1^+ + R_2$$

(2.b) Dissociative ionization

$$R_1R_2 + h\nu \rightarrow R_1^+ + R_2 + e^-$$

(3) Pre-ionization of the excited molecule

$$R_1R_2 + h\nu \rightarrow R_1R_2^* \rightarrow R_1R_2^+ + e^-$$

The energy thresholds for these processes are, in general, different and the one for the simple ionization (1.a) and (1.b) corresponds generally to the lowest energy; but this may not be always the case. For molecules containing atoms of high electron affinity, the photoionization process most likely to occur at the first threshold could be dissociation into ions. This phenomenon was demonstrated in the early 1930's by Terenin and Popov [1] for thallium halide vapours, which split into $Tl^+ + Hal^-$ as a primary photo process. Later, Morrison et al[2] have

shown a similar process for Br_2 and I_2, where the first threshold corresponds to a pre-ionization accompanied by the dissociation.

$$Br_2 + h\nu \longrightarrow Br_2^* \longrightarrow Br^+ + Br^-$$

and

$$I_2 + h\nu \longrightarrow I_2^* \longrightarrow I^+ + I^-$$

Besides the processes described above leading to charged particles, there are probably others giving neutral radicals but these are not detected in a mass spectrometer. One of the methods to distinguish between the different processes is by studying the photoionization yield curves and from these extract the values of the photoionization cross-sections of atoms and molecules and of the adiabatic and vertical ionization potentials.

The absolute photoionization quantum yield A in ions per photon is the ratio of the ion current i to the amount of

absorbed radiation Io-I where Io and I are respectively the light fluxes of the incident and transmitted radiation in the ionization region. The product of the absolute photoionization quantum yield A and the total effective absorption cross-section σ is the effective photoionization cross-section σ_i, sometimes called simply photionization efficiency. It is shown that, when the pressure of the gas being studied is low (10^{-3} - 10^{-5} torr) the photoionization cross-section σ_i can be given by the ratio of the ion current to the incident light flux in photons per second.

Thus $$\sigma_i = C \frac{i}{I\partial}$$

where C is a constant depending on the instrumental porameters.

In order to obtain reliable values for ionization potentials, the shape of the photoionization efficiency curves has to be carefully interpreted. Watanable [3,4] has

discussed in detail these curves near the appearance threshold of the ion current and has established a criterion to extract the adiabatic ionization potentials from them.

However, Watanabe could not identify unequivocally the ions produced in the photoionization processes as he did not use mass analysis. This was obviated by a combination of the monochromator with a mass spectrometer.[5-7] Even so, in the ionization of complex molecules, the efficiency curves became quite difficult to interpret as there is a smearing-out of the abrupt jumps in the ion current, owing to the great number of vibrational levels involved.

A more recent method of determing ionization potentials and ionic energy levels is by photo-electron spectroscopy.[8-11] Our instrument can be used as a coincidence photo-electron spectrometer if a retarding field is introduced near the ionization chamber, parallel to the electron trajotories and before the electron collector. The retarding field would be given by two flat grids, the nearest to the ionization

chamber at potential V and the next one at ground potential, as is shown in fig. 19.

It is possible that plate No. 1 needs to have a small draw-out potential [12] to decrease the spread in the flight times. Plate No. 2 would be kept as it stands for normal operation.

When a photon of energy $h\nu$ impacts a molecule, the excess energy of that required to produce ionization is taken by the ejected electron as kinetic energy.

Hence,

$$h\nu = IP + KE$$

and

$$IP = h\nu - KE$$

If the voltage V is scanned, increasing by fine steps from zero, the curve plotted with increasing potential V, against the number of electrons overcoming the potential barrier and so reaching the electron detector, should

by plotting the number of coincidences corresponding to that particular delay time, vs the increasing retarding potential.

3.2 COINCIDENCE TECHNIQUE

The application of the coincidence technique to the measurement of disintegration rates was a simple absolute method practised in nuclear physics since the 1930's [13]. In order to get better accuracy, the initial simple formulae were corrected to a more complex presentation but the coincidence method still remains an absolute method with high sensitivity.

The application of this technique to mass spectrometry was only recently described by Rosenstock[14] and after by Vestal [15] and Brehm and Puttkamer.[16]

Suppose the number of ionization events in the ionization region, from which ions and electrons are

collected, is N_z and F_e and F_i respectively are the fractions of electrons and ions collected. Then the number of ejected electrons from the ionized molecules arriving per second at the collector is

$$N_e = F_e N_z$$

and the corresponding number of ions per second collected in the ion detector is

$$N_i = F_i N_z$$

An ionization event is only detected in the delayed coincidence method if both electronand ion are collected simultaneously. So, the number of true coincidences per second is a fraction of the ionization events given by

$$N_c = F_e F_i N_z$$

The electron collector, in addition to the true electron pulses, N_e per second, may detect N_p pulses from electrons extracted from the walls by photoelectron effect and from direct detection of ultraviolet radiation, although this would account for a small percentage, owing to the detector characteristics. Also, N_n random noise pulses produced in the multiplier by sources as cosmic rays. Thus, the total number of pulses in the electron detector per second, or the electron detector counting rate is N'_e

$$N'_e = N_e + N_p + N_n$$

$$= F_e N_z + N_p + N_n \qquad (1)$$

As, in general, there is no source of stray ions, the total number of pulses at the ion collector per second or the ion detector counting rate is :

$$N_i' = N_i + N_m = F_i N_z + N_m \qquad (2)$$

where N_m is the noise pulses of the ion detector.

If τ_R is the coincidence unit resolving time, for proper operation of the coincidence mass spectrometer the product $N_e' \tau_R$ must be less than unity.

Consider the random coincidences or background[17] gained owing to the finite value of the coincidence unit resolving time τ_R. If N_e' and N_i' are the observed counting rates at the electron and ion channels respectively, the number of pulses at the electron channel which did not give rise to a true coincidence is simply:

$$N_e' - N_c$$

and the random or background coincidence rate due to these pulses is

$$(N_e' - N_c) \quad N_i' \tau_R.$$

Similary, the random rate /

associated with the ion-channel counting rate corrected for true coincidences is

$$(N_i' - N_c) \; N_e' \tau_R$$

Then the total random coincidence rate is given by

$$N_R = (N_e' - N_c) \; N_i' \; \tau_R + (N_i' - N_c) \; N_e' \; \tau_R$$

$$= \tau_R \left[2 \, N_e' \, N_i' - (N_e' + N_i') \, N_c \right] \qquad (3)$$

The ratio of random coincidence rate or background to the true coincidence rate is

$$B = \frac{N_R}{N_c} = \frac{\tau_R \left[2 \, N_e' \, N_i' - (N_e' + N_i') \, N_c \right]}{F_i F_e N_z}$$

and replacing N_e' and N_i' by eq. (1) and (2)

$$B = \frac{N_z \tau_R \left[2\left(F_e + \frac{N_p + N_n}{N_z}\right)\left(F_i + \frac{N_m}{N_z}\right) - \left(F_e + F_i + \frac{N_p + N_n + N_m}{N_z}\right) F_i F_e \right]}{F_i F_e} \qquad (4)$$

As from eq. (4) the noise to signal ratio is a function of the ionization rate N_z. In non-coincident mass spectrometers, the maximum sensitivity is limited by the constant noise level, as signal and noise levels are independent. The coincident mass spectrometer, by the opposite, possesses this important characteristic of absolute sensitivity.

We considered in expression (3) the random coincidences generated from the resolution time τ_R of the coincidence unit. There is, however, another factor that modifies the coïncidence ratio, causing a loss of coincidences.

Suppose τ_D is the dead time imposed on both ion and electron channel input pulses; normally τ_D is bigger than τ_R.

Following the method of Hayward[18] the rate of lost coincidences is given by

$$N_c N_z \left\{ F_e F_i \tau_D + (\tau_D - \tau_R) \left[F_i(1 - F_e) + F_e(1 - F_i) \right] \right\} \quad (5)$$

As shown by eq. (3), (4) and (5), it is very important to have the resolution time of the coincidence unit τ_R, and the "dead time" of the input channels τ_D, as low as possible to get the maximum sensitivity, or maximum signal to noise ratio in the coincidence mass-spectrometer.

3.3. TRAVEL TIME OF IONS AND CONSIDERATIONS ON RESOLUTION

The travel time of an ion in this instrument is obtained by solving the equations of motion of a charged particle in a uniform electrostatic field.

If ions are accelerated through a potential difference V, and travel the distance L in the field direction, the normal travel time of an ion species of a given mass-to-charge

ratio $\left(\frac{m}{e}\right)$ is :

$$t_m = L \left(\frac{2m}{eV}\right)^{\frac{1}{2}} \qquad (1)$$

Eq. (1) is deduced from the following set of equations.

$$eV = FL$$

$$F = mj$$

$$L = \tfrac{1}{2} j t^2$$

When t is measured in μ sec, L in cm, m in a.m.u. and V in volts expression (1) becomes

$$t_m = 1.44 \left(\frac{m}{V}\right)^{\frac{1}{2}} \times L \qquad (2)$$

or

$$t_m = 1.44\, m^{\frac{1}{2}} \left(\frac{L}{E}\right)^{\frac{1}{2}} \qquad (3)$$

where $E = \frac{V}{L}$ is the electrostatic field in volts per cm.

The main difficulties for obtaining high resolution come from the spread in flight times owing to the variations in initial position and kinetic energy of ions formed in the source.

For an ion with a velocity component in the direction of the acceleration field, corresponding to aninitial kinetic energy Vo in e.v., the total travel time is given by expression (4)

$$t_m\ (\ Vo) \ = \ 1.44\ m^{\frac{1}{2}} \quad \frac{(Vo\ + EL\ )^{\frac{1}{2}} \pm (Vo)^{\frac{1}{2}}}{E} \qquad (\ 4\ )$$

The plus and minus sign in Vo corresponds to the case in which the ion is formed with the initial velocity directed away from the ion detector, or towards the ion detector respectively.

The total variation in the ions flight time, owing to the initial kinetic energy Vo is the time needed for an ion formed with initial kinetic energy Vo, directed away from

the ion detector to return to its original position. In what follows we calculate the time spent in the "turn-around".

Suppose the ion is formed in position P with kinetic energy Vo, in opposite direction to the field E, i.e. directed away from the ion detector.

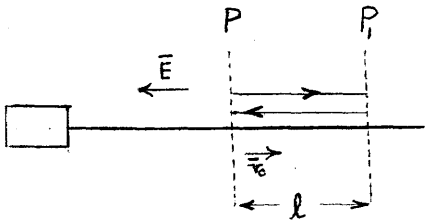

This means that the ion will have a velocity vo given by

$$Vo = \tfrac{1}{2}\, m\, vo^2 \qquad (5)$$

then

$$vo = \left(\frac{2\,Vo}{m} \right)^{\frac{1}{2}} \qquad (6)$$

The ion will take a time t to travel the distance l in the direction of the initial velocity with uniformly retarded motion until the moment it turns round in the direction of the field E.

$$F = m\,j$$

$$F = e\,E \quad \therefore \quad j = \frac{eE}{m} \qquad (7)$$

$$\frac{d\,l}{d\,t} = v = v_o - j\,t = 0$$

$$v_o = j\,t \quad \therefore \quad t = \frac{vo}{j} \qquad (8)$$

If in eq. (8) we replace v_o and j by e.g. (6) and (7) respectively we get

$$t = \frac{\sqrt{2}}{eE} \left(m\,Vo \right)^{\frac{1}{2}}$$

or

$$t = \frac{1.44}{E} \left(m\,Vo \right)^{\frac{1}{2}} \qquad (9)$$

As the ion takes the same time t to come from P_1 to P ; the total time spent for the "turn around" is :

$$\Delta t \ (Vo) = \frac{2.88}{E} (mVo)^{\frac{1}{2}} \qquad (10)$$

When ions are formed with no kinetic energy there are still fluctuations in travel time owing to the variations in initial position; as they can be formed along all the width of the ionizing beam.

If the width is ΔL the fluctuation due to initial position will be given by differentiation of eq. (2)

Hence

$$\Delta t_m \ (\Delta L) = 1.44 \left(\frac{m}{V}\right)^{\frac{1}{2}} \Delta L. \qquad (11)$$

To define mass resolution we need to calculate the difference in travel times for two adjacent masses m + 1 and m.

$$\Delta t_m = t_{m+1} - t_m = 1.44 \left(\frac{m}{V}\right)^{\frac{1}{2}} \times L \times \left[\left(1 + \frac{1}{m} \right)^{\frac{1}{2}} - 1 \right] = \frac{tm}{2m} \qquad (12)$$

present a series of steps corresponding to the discrete values of adiabatic and vertical potentials.

In the way described above, only the electron channel is used without coincidence and so the particular ion species where the electrons come from are not simultaneously mass identified.

However, our instrument is able at the same time to mass analyse, meaning that the actual electron stopping curves would correspond only to a particular ion species identified by the coincidence time-of-flight analysis technique,

This is done by first running a spectra of the compound in study, to identify the ions present. After that, the delay time of the electron pulses (equivalent to ion flight times) is kept on the appropriate value to collect, in coincidence, only, the ions of the desired mass. The ionization potentials and hence the energy levels of the excited ions would then be taken from the curve obtained

Then comparing eq. (10) with eq. (12) the higher mass that can be resolved owing to travel time fluctuations arising from the initial kinetic energy is:

$$m(Vo) = \frac{1}{4} \times \left(\frac{V}{Vo} \right)^{\frac{1}{2}} \qquad (13)$$

In the same way, comparing eq. (11) with eq. (12) shows that the higher mass which can be resolved due to variations in initial position is

$$m\ (\Delta L) = \tfrac{1}{2} \times \frac{L}{\Delta L} \qquad (14)$$

The values calculated above did not take into consideration the loss in resolution arising from the electronic units, such as the limitation derived from the coincidence unit resolution time τ_R, and the smallest available delay increments in the delay line.

3.4 THE APPLICATION OF THE COINCIDENCE TIME-OF-FLIGHT MASS SPECTROMETER TO DIRECT DETERMINATIONS OF METASTABLE LIFE-TIMES

Some ions formed in the mass spectrometer are just long-lived enough to decompose somewhere in the middle of their flight along the tube.

Since the early work of Hipple [19], many workers gathered information about life-times of metastable ions.

Very sensitive means of detection specially designed for metastable ion analysis have been developed .

Hipple in his original work explained the curves obtained, assuming that there were two processes with two different life-times. Momigny [20] repeated this work and has concluded this also; namely the existence of two different life-times.

Later Coggeshall[21] for the same decomposition calculated three transitions with three life-times, although Schug[22] demonstrated that the three values could be represented also by only two with the same precision. So, no definite

conclusion as whether two or three life-times were involved, was possible.

Ottinger[23] built an apparatus in which the ions are formed and accelerated in a well defined electric field afterwards being subjected to electrostatic energy analysis and magnetic mass analysis. By varying the electrostatic field, information can be obtained through the kinetic energy of the fragments, about the time interval between the ionization of a molecule and its dissociation.

The experiments of Ottinger have shown that there is a quite smooth non-linear decrease of metastable intensity with time, which is a sign that a large number of life-times are involved in a continuous distribution.

However, more information about metastable life-times is still necessary. The coincidence time-of-flight mass spectrometer in principle is able to give the life-times of the metastable ions observed in the spectrum. However, for that purpose it would be necessary that the resolution of the

particular apparatus used, allows a separation of the peaks corresponding to the parent, fragment and metastable ions.

Let L be the distance between the axis of the ionizing beam P and the ion collector, and L_1 the distance between P and the point along the flight tube where the decomposition of the ion of mass m_1 has occurred.

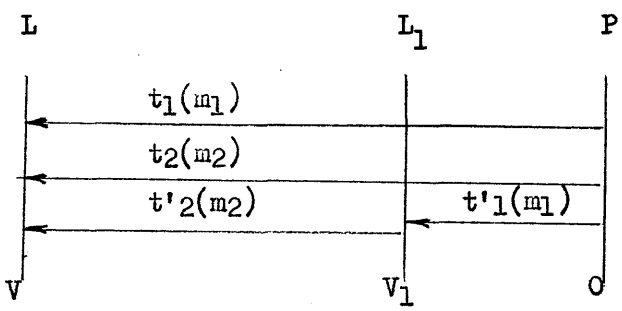

An expression that allows the calculations of the mean life-time of the decomposing ion can be calculated.

Discriminating as follows the several flight times involved in the process:

t_1 - mass m_1 from P to L

t_2 - mass m_2 from P to L

t_1' - mass m_1 from P to L_1

t_2' - mass m_2 from L_1 to L,

$t_1' + t_2' = T$

the initial velocity of the ion of mass m_2 at the point L_1, has to be considered for the calculation of t_2'.

The equations involved in the calculations are the following:

$$\frac{t_1}{t_2} = \left(\frac{m_1}{m_2} \right)^{\frac{1}{2}} \qquad (1)$$

$$\frac{L}{L_1} = \frac{V}{V_1} \qquad (2)$$

$$L - L_1 = \left(\frac{2e\,V_1}{m_1}\right)^{\frac{1}{2}} t_2' + \tfrac{1}{2}x\left(\frac{2e\,(V - V_1)}{m_2}\right)^{\frac{1}{2}} t_2' \qquad (3)$$

$$t_1' + t_2' = T \qquad (4)$$

$$\frac{t_1}{t_1'} = \frac{L}{L_1} \times \left(\frac{V_1}{V}\right)^{\frac{1}{2}} \qquad (5)$$

Working out those five equations we obtained the following expression

$$\alpha L_1^{\frac{1}{2}} - L_1 + \left(\gamma - \delta L_1\right)^{\frac{1}{2}} - \left(\beta L L_1 - \beta L_1^2\right)^{\frac{1}{2}} - L = 0 \qquad (6)$$

where

$$\alpha = \left(\frac{2\,e\,V}{m_1 L}\right)^{\frac{1}{2}}$$

$$\beta = \left(\frac{t_1}{t_2}\right)^2$$

$$\gamma = \left(\frac{T^2 e V}{2 m_2} \right)$$

$$\delta = \left(\frac{T^2 e V}{2 m_2 L} \right) = \frac{\gamma}{L}$$

Eq. (6) can be solved by numerical approximation. The values of L_1 obtained must be positive and smaller than L.

The values of L_1 are after substituted in the eq.

$$t_1' = L_1 \left(\frac{2 m_1}{e V_1} \right)^{\frac{1}{2}}$$

which should give the values for the mean life-time of the metastable ion.

REFERENCES

1. A.N.TERENIN and B.POPOV, Physik.Z.Sowjetunion, 2 (1932) 299.
2. J.D.MORRISON, H.HURZELER and M.G.INGHRAM, J.Chem.Phys., 33 (1960) 821.
3. K.WATANABE, J.Chem.Phys., 22 (1954) 1564.
4. K.WATANABE, J.Chem. Phys.,26 (1957) 542.
5. H.HURZELER, M.G.INGHRAM and J.D.MORRISON, J.Chem.Phys., 28 (1958) 76.
6. G.L.WEISSLER, J.A.R.SAMSON, M.OGAWA and G.R.COOK, J.Opt.Soc.Am., 49 (1959) 338.
7. V.H.DIBELER and R.M.REESE, J.Res.Nat.Bur.Stand., 68a (1964)409.
8. D.W.TURNER, and M.I.AL-JOBOURY, J.Chem.Phys., 37 (1962) 3007.
9. R.I.SCHOEN, J.Chem.Phys., 40 (1964) 1830.
10. D.C.FROST, C.A.McDOWELL, J.S.SANDHU and D.A.VROOM, "Advan.Mass Spectry." 4, Institute of Petroleum, London (1968) 781.
11. B.BREHM and E.von PUTTKAMMER, Z.Naturf., 22a (1967) 8.
12. B.BREHM and E.von PUTTKAMMER, "Advan.Mass Spectry." 4 , Institute of Petroleum, London (1968) 591.

13. B.ROSSI, Nature, 125 (1930) 636; W.BOTHE, Z.Physik,59 (1930) 1.

14. H.M.ROSENSTOCK, U.S. Patent 2 999 157 (1961).

15. M.L.VESTAL, U.S. Patent 3 307 033 (1967); M.L.VESTAL, M.KRAUSS, A.L.WAHRHAFTIG and W.H.JOHNSTON, A.S.T.M. Committee E-14 , 11th Annual Conference, S.Francisco (1963).

16. B.BREHM and R.von PUTTKAMMER, "Advan.Mass Spectry." 4, Institute of Petroleum, London (1968) 591.

17. P.J.CAMPION, Int.J.Appl.Rad.Isotopes, 4 (1959) 232.

18. R.W.HAYWARD, Int.J.Appl.Rad.Isotopes, 12 (1961) 148.

19. J.A.HIPPLE, Phys.Rev., 71 (1947) 594.

20. J.MOMIGNY, Bull.Soc.Chim.Belge, 70 (1961) 291.

21. N.D.COGGESHALL, J.Chem.Phys., 37 (1962) 2167.

22. J.C.SCHUG, J.Chem.Phys., 40 (1964) 1283.

23. C.OTTINGER, Z.Naturf., 22a (1967) 20.

24. N.R.DALY, A.McCORMICK and R.E.POWELL, Rev.Sci.Instr., 39(1968)1163.

Chapter Four

EXPERIMENTAL RESULTS AND DISCUSSION

With the present equipment, the resolution of the spectrometer is low.

In the coincidence unit used (type 1036 C) the smallest resolution time τ_R available is 0.1 μ s; this means that mass peaks corresponding to ion species with travel times differing in 0.1 μ sec or less cannot be resolved.

As L is approximately 20 cm, and using 2000 V for ion acceleration, the nominal travel time of an ion of mass m is

$$t_m = \frac{1.44 \times 20}{(2000)^{\frac{1}{2}}} \times m^{\frac{1}{2}}$$

or

$$t_m = K \times m^{\frac{1}{2}}$$

where

$$K = .644$$

The maximum resolvable mass allowed by the coincidence unit resolution time τ_R is calculated by application of expression (12) in paragraph 3.3.

As $$\Delta t = \frac{t_m}{2m} \qquad (1)$$

If $$t = .1\ \mu \text{ sec.}$$

and

$$t_m = K \times m^{\frac{1}{2}}$$

we get

$$.1 = \frac{K\, m^{\frac{1}{2}}}{2m}$$

then $$m \approx 10$$

The maximum resolution, at present is therefore, 10.

In the spectrum shown in fig. 19, the travel time of the two peaks present can be taken as 6.3 and 7.5 μ sec.

The ion acceleration during those experiments was kept constant at -2000 V, and so we can use the above calculated

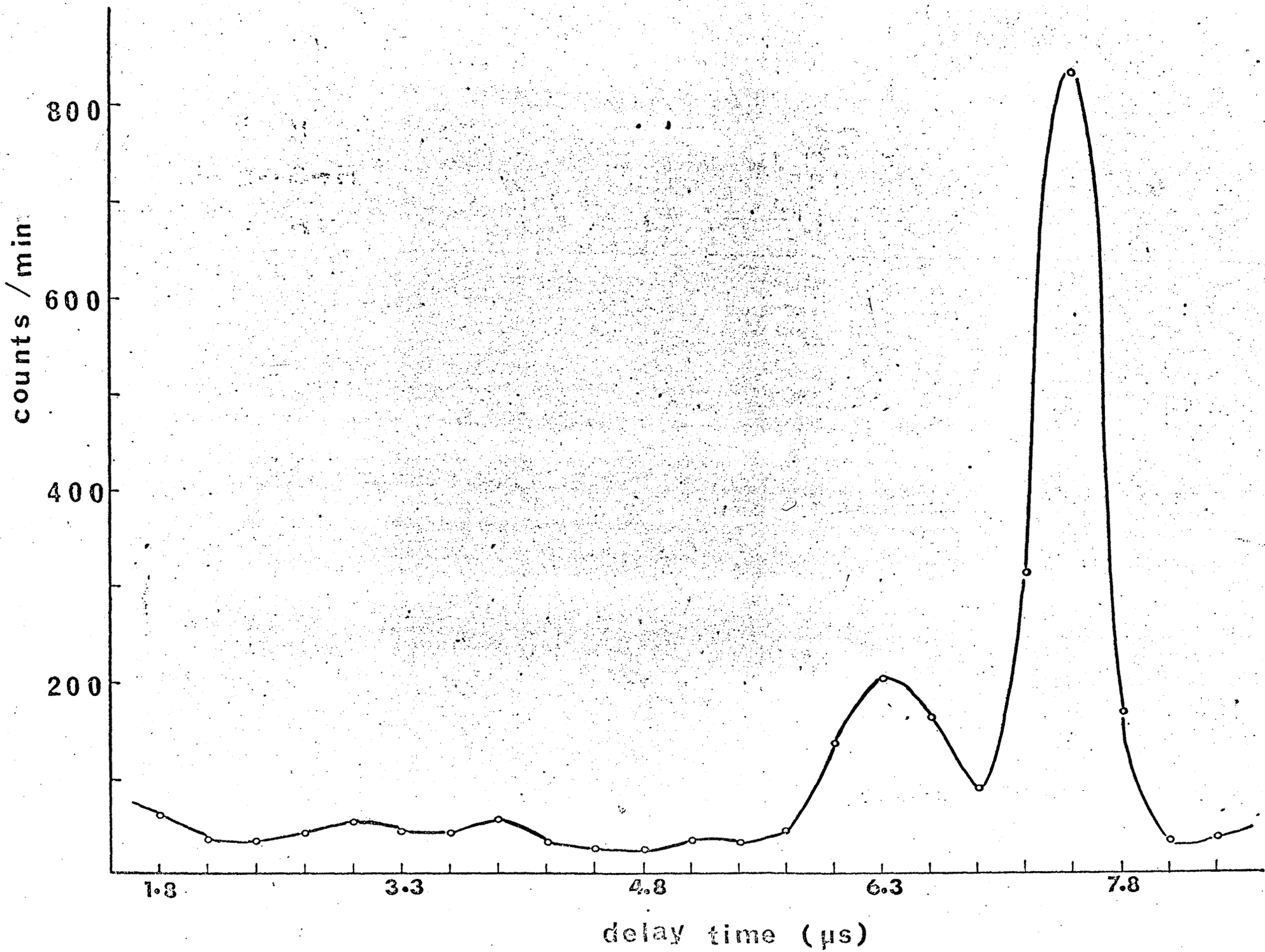

FIG.19

Figure	VOLTAGES (V)				PULSE AMPLIFIERS (type 652)								COINCID. UNIT Resolving time (μsec)	LIGHT SOURCE Intensity (divisions)	PRESSURE (10^{-6} torr)	
	DETECTORS		ACCELER.		RISE TIME (μsec)		FALL TIME (μsec)		ATTENUAT (dB)		DISCR. VOLT (V)				backg	sample
	electr	ion	electr	ion	elect	ion	electr	ion	electr	ion	elect	ion				
19	3100	2800	350	2000	.1	.1	1	1	8	0	9	6	.4	5.6	2.5	7
20	3100	2800	350	2000	.1	.1	1	1	2	0	10	6	.4	6.0	2.5	7
21	3000	2800	350	2000	.1	.1	1	1	2	0	10	6	.1	6.1	2.5	7
22	3000	2800	35o	2800	.1	.1	1	1	0	0	10	6	.1	5.5	2.5	8
23	3000	2800	350	2000	.1	.1	1	1	0	0	10	6	.4	2.0	2.5	7.8

TABLE I

constant (K = .644), for the ion mass determination as follows:

$$\text{for } t = 7.5\ \mu\text{ sec.} \quad m^{\frac{1}{2}} = \frac{7.5}{.644} = 11.64$$

or

$$m = 135.5 \text{ a.m.u.}$$

and for $t = 6.3\ \mu$ sec.

$$m^{\frac{1}{2}} = \frac{6.3}{.644} = 9.78$$

or

$$m = 95.6 \text{ a.m.u.}$$

The instrumental parameters in the experiment of fig. 19 are specified in table I.

Those deduced masses were quite unexpected, as the sample introduced in the inlet system was 1 - 1 - 1 trifluorethane (m = 84), which molecular ion corresponds to a travel time of 5.9 μ sec.

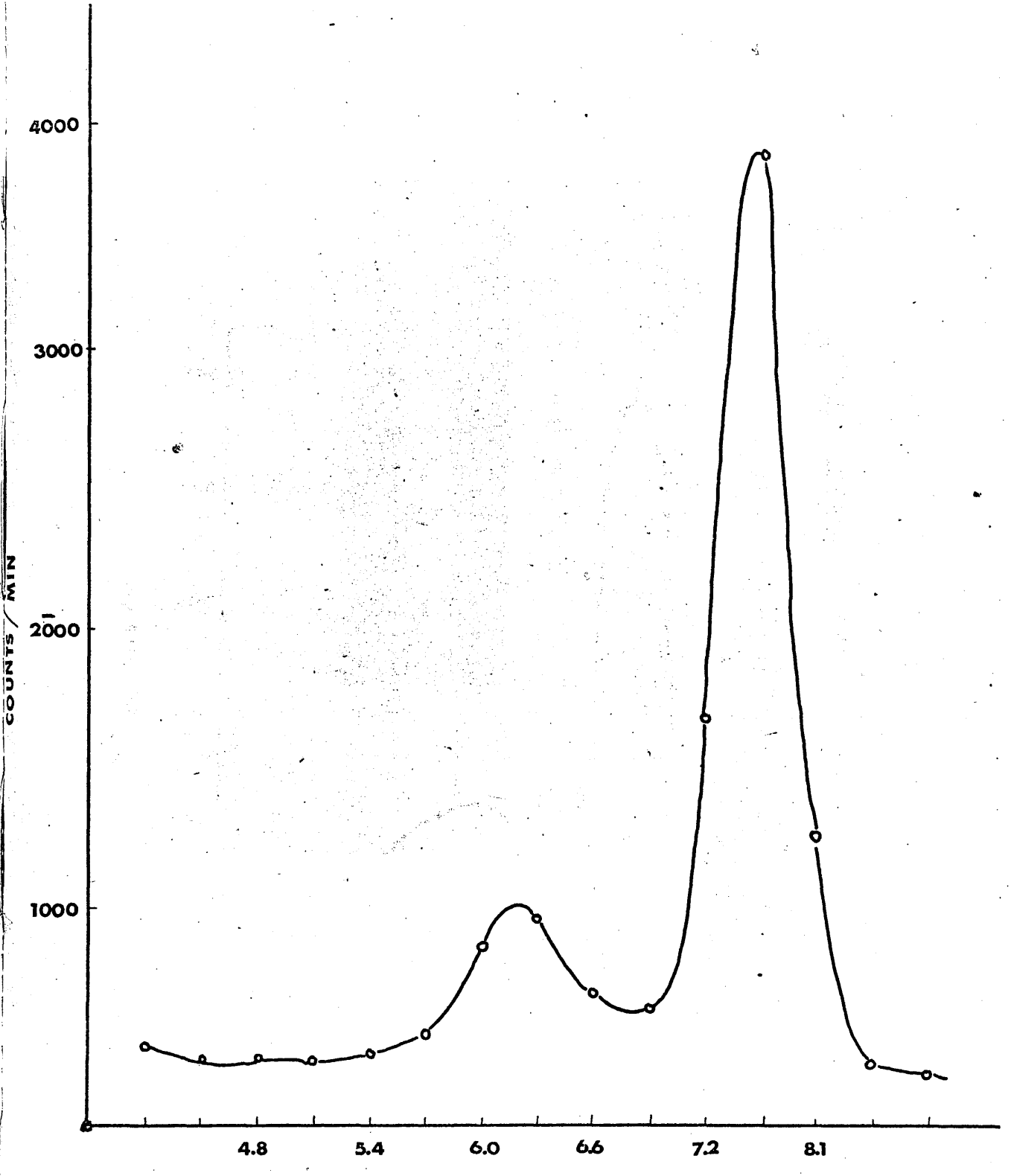

FIG. 20

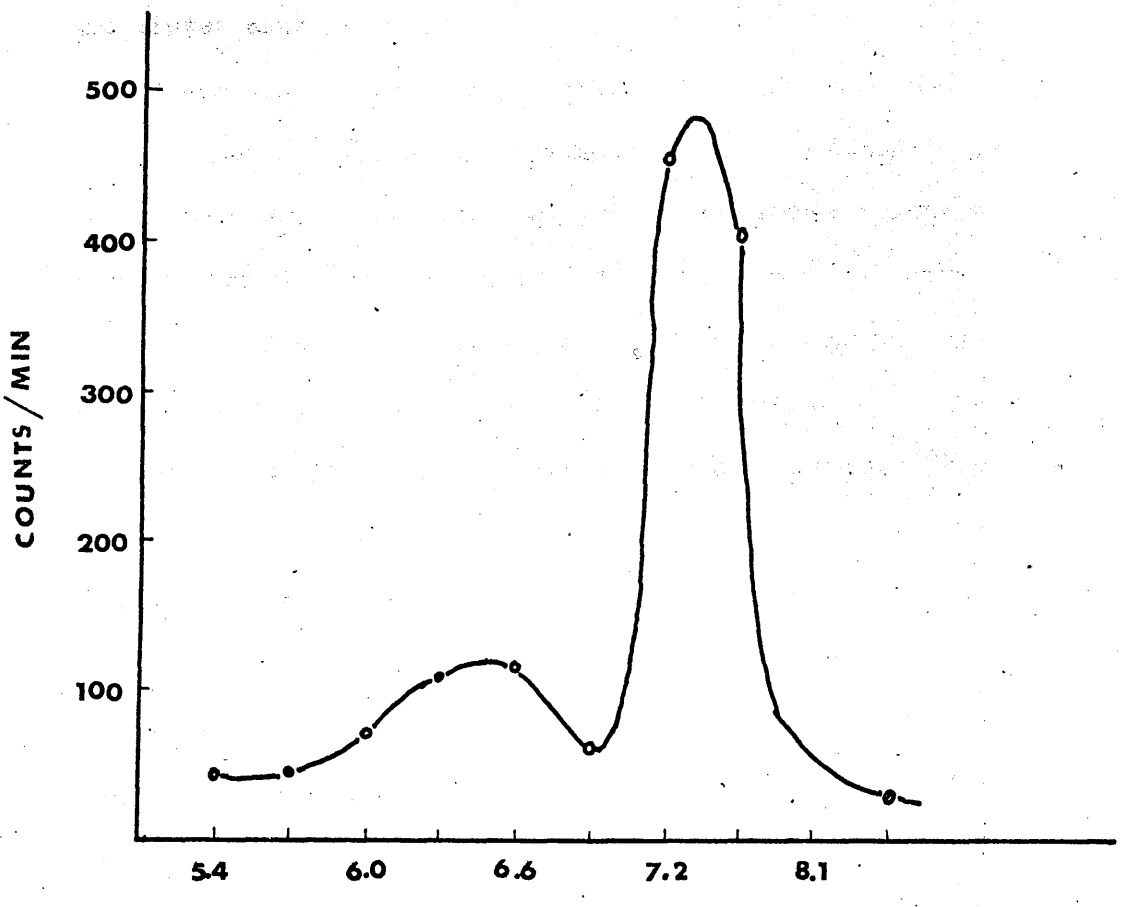

FIG. 21

However, the spectrum was quite reproducible as can be seen in figs. 20 and 21 for which the experimental conditions are listed also in table 1.

There was the possibility that those peaks had come from cracked pumping oil, as the system had been accidentally let up to atmosphere while pumping. To confirm this hypothesis a small sample of oil was pyrolised, in contact with air, and ~~the issuing contact with air, and~~ the issuing vapours trapped and analysed in the AEl - MS9 mass spectrometer.

The resulting spectrum presented peaks at masses 91,92, 93,94 and 95 in a group, and 133 and 135 in another, which are in fair agreement with the above calculated values. This confirmed the origin of the peaks.

A gross estimate of the resolution for this spectrum, taking into account the large mass separation of the two peaks, was about 3. This was again in fair agreement with the theoretical value, as the coincidence unit's resolution time had been set at 0.4 μ sec. (eq. 1).

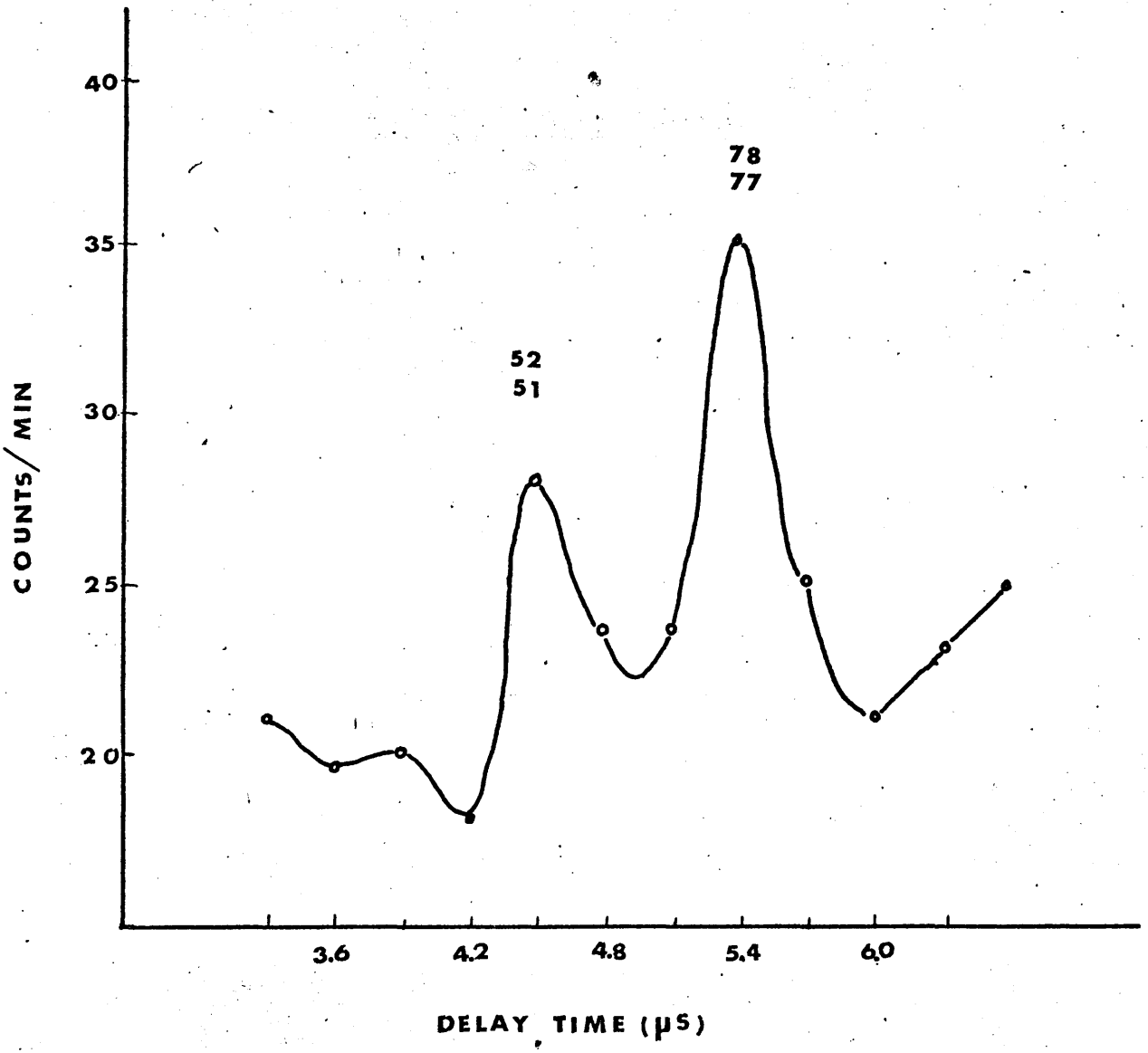

FIG. 23

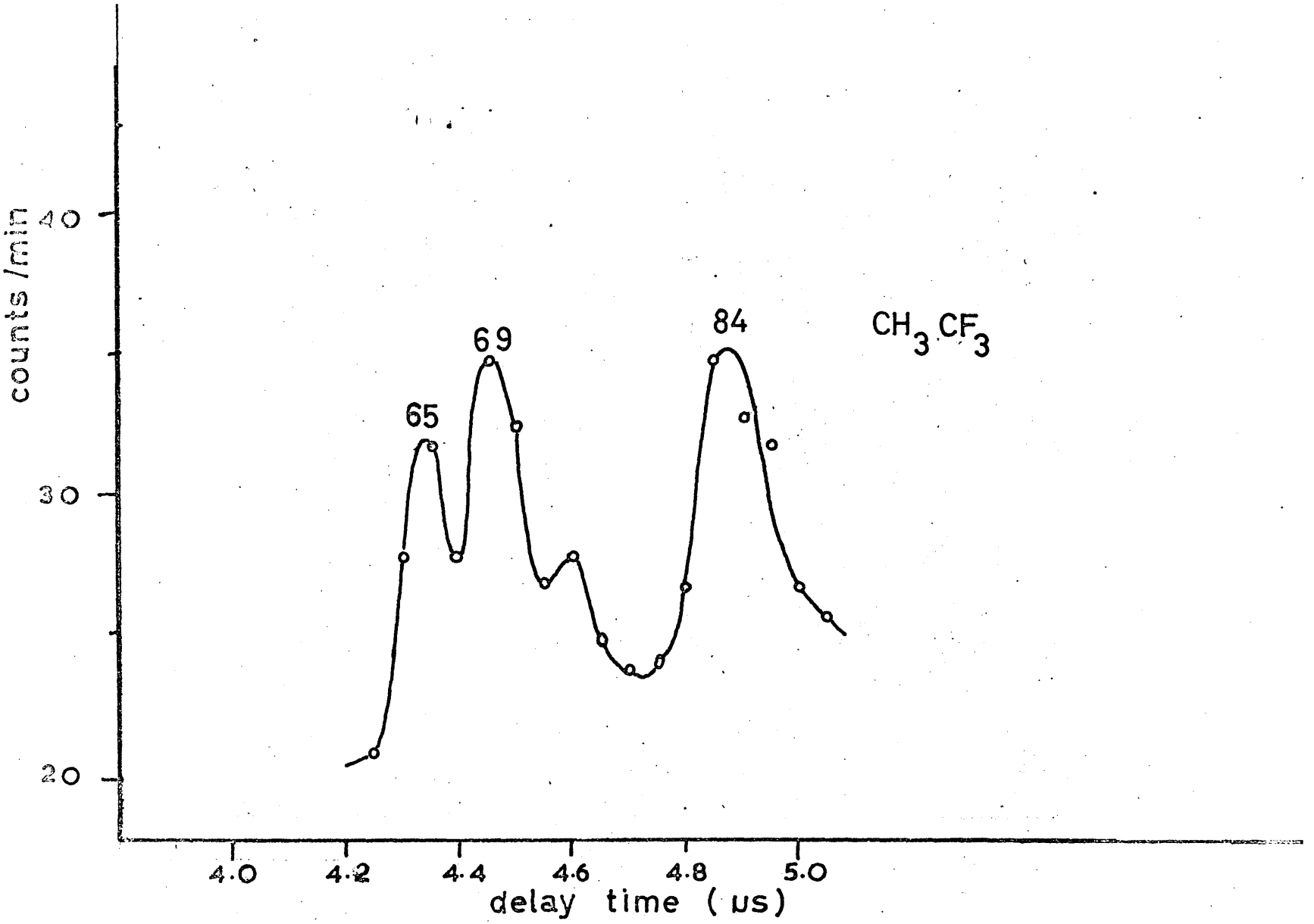
counts /min
40
30
20
65
69
84
CH_3CF_3
4.0
4.2
4.4
4.6
4.8
5.0
delay time (μs)

FIG. 22

A spectrum of the 1 - 1 - 1 trifluorethane was later obtained and is shown in fig. 22. Fig. 23 shows the spectrum of benzene.

All the corresponding parameters are shown in Table 1.

C O N C L U S I O N S

Before further investigations could be pursued it is necessary to increase the resolution. For that purpose, besides the improvement in the electronic units involved, it would be advantageous to add an extension to the flight tube and to increase the number of plates, so that the potential gradient would become less steep.